1.0 INTRODUCTION

The standard electroweak interaction model[1], based on broken SU(2)×U(1) symmetry has been very sucessful in fitting all of the presently available data. Indeed this model even predicted many of the data's features. It predicted the existence of a $\Delta S=0$ neutral current even though strangeness changing neutral currents were limited by experiment to be very small. Since the weak neutral current was discovered[2] in neutrino scattering, very detailed meassurements[3] have been made of its structure, particularly by scattering neutrinos off quarks. All of the data from these experiments can be fit to the original model with its one free parameter, $\sin^2\theta_w$. Data from the purely leptonic process, neutrino electron scattering[4], also are fit by the model with the same value of $\sin^2\theta_w$. Finally, a very high precision measurement[5] of parity violation in electron deuteron scattering also was in good agreement with the model and determined the SU(2) multiplet structure of the fermions to be as originally expected.

The low energy limit of the model has therefore been tested very stingently by the combination of all of these experiments. However, some of its most interesting features, such as spontaneous symmetry breaking and the existence of intermediate vector bosons at predicted masses, are not yet tested by the data. As was first pointed out by Bjorken[6], all that is needed to fit the data is a global SU(2) symmetry, weak electromagnetic mixing and universality. The new measurements needed to pin down these important predictions of the GWS model are to find the scalar particles responsible for symmetry breaking and to make measurements at high q^2 where the boson structure of the interaction may be determined.

---

1 S.L. Glashow, NP 22 (1961) 579; Rev. Mod. Phys. 52 (1980) 539. A. Salam, Phys. Rev. 127 (1962) 331; Rev. Mod. Phys. 52 (1980) 525. S. Weinberg, Phys. Rev. Lett. 19 (1967) 1264; Rev. Mod. Phys. 52 (1980) 515.

2 F.J. Hasert et al., Phys. Lett. 42B (1973) 121.

3 K. Winter, Proc. of the 1979 International Symposium on Lepton and Photon Interactions, Fermilab (1979) p. 258; P. Langacker et al., Proc. of Neutrino 79, Bergen, (1979), p. 276.

4 H. Faissner, New Phenomena in Lepton-Hadron Physic (1979), ed. D. E. Fries and J. Wess (Plenum Publishing Corp., New York), p. 371. F. W. Bullock, Proc. of Neutrino 79, Bergen 1979, p. 398. R. H. Heisterberg et al., Phys. Rev. Lett. 44 (1980) 635. L. W. Mo, Contribution to Neutrino 80, Erice (1980). M. Roos and I. Liede, Phys. Lett. 82B (1979) 89, and references therin. F. W. Büsser, Proc. of Neutrino 81, Wailea, Hawaii (1981).

5 C.Y. Prescott et al., Phys. Lett. 77B (1978) 347.

On the surface it seems that a theory that made so many predictions which were subsequently verified, would be very likely to be correct. However the large number of parameters in the Higgs sector has seemed unnatural to many and has spawned further searches for models that do not contain so many parameters yet naturally explain the low energy data. These models include GUTs, technicolor models, supersymmetric GUTs and constituent models. Many of these models yield a different high energy behavior than GWS.

To be more specific, several authors[7] have proposed alterations to the standard model which would give a different boson structure. The least radical change among these has first been proposed by Georgi and Weinberg. They showed that by extending the symmetry group from $SU(2)\times U(1)$ to $SU(2)\times U(1)\times G$, which may be embedded in a larger symmetry group in a GUTs model, all of the low energy predictions of the model remain unchanged. At high energy, however, the extended models have a richer boson structure. A more radical example of a model is one where the W's, Z's and fermions are composed of constituents and, at energies of the order of 1 TeV, a continuum of weak interactions occur. At low energies in these models, weak interactions may be dominated by the lowest lying resonance, an analogous situation to vector dominance in the strong interactions of the photon where the ρ meson is a bound state of constituent quarks.

At low energy, all of the models, including the standard one, can be described by an effective neutral current Hamiltonian

$$2H_{NC} = \frac{-e^2}{q^2} j_{EM}^2 + \frac{8G_F}{\sqrt{2}} \left[(j^{(3)} - \sin^2\theta_W \cdot j_{EM})^2 + C \cdot j_{EM}^2 \right] \qquad (1)$$

where $j^{(3)}$ is the third component of the weak isospin current.

---

[6] J. D. Bjorken, Unification of Elementary Forces and Gravitation (Hartwood Academic Publishers, London 1978)p. 701; Proc. of the 13th Rencontre de Moriond, ed. Tran Thanh Van, p. 191; Phys. Rev. D19 (1979) 335; compare also the recent review, FERMILAB-Conf-80/86 THY (1980). P. Q. Hung and J. J. Sakurai, Nucl. Phys. B143 (1978) 81.

[7] H. Georgi and S. Weinberg, Phys. Rev. D17 (1978) 275. V. Barger, W. Y. Keung and E. Ma, Phys. Rev. Lett. 44 (1980) 1169. E. H. deGroot, D. Schildknecht and G. J. Gounaries, Phys. Lett. 90B(1980) 427. E. H. de Groot and D. Schildknecht, Phys. Lett. 95B (1980) 149.

$$\vec{J}_\mu = \sum \bar{\psi}_i \gamma_\mu (1-\gamma_5)/2 \vec{\tau}/2 \psi_i \qquad (2)$$

with the sum running over all weak fermion doublets. In the standard model, as in any model with a single Z boson, the constant C is equal to zero. In theories with more than one Z boson, C will be greater than zero.

Gounaris and Schildknecht[8] have given a nice interpretation of the parameter C in terms of a deviation from the standard model. They found

$$16\ C = \frac{\left[\int ds\ s\cdot\sigma(e^+e^-\to ALL)\right]_{ACTUAL} - \left[\int ds\ s\cdot\sigma(e^+e^-\to ALL)\right]_{GWS}}{\left[\int ds\ s\cdot\sigma(e^+e^-\to ALL)\right]_{GWS}} \qquad (3)$$

so that the quantity 16 C measures the deviation of the total $e^+ e^-$ cross section from the standard model, integrated over all energy with the weighting factor 1/s. C will therefore be a parameter of general interest to weak interaction model builders.

Throughout the paper, I will describe the strength of the axial vector and vector couplings of the weak neutral current in terms of the dimensionless coupling constants g_A and g_V. In the standard model we have for the left handed fermion doublets under weak SU(2)

$$\begin{aligned} g_A &= T_3 \\ g_V &= T_3 - 2\cdot q\cdot \sin^2\Theta_W. \end{aligned} \qquad (4)$$

In the weak part of the Hamiltonian of equation (1), the axial vector-axial vector term is proportional to g_A^2, the axial vector-vector term is proportional to $g_A g_V$, and the vector-vector term is proportional to $g_V^2 + 4C$.

---

[8] G. J. Gounaris and D. Schildknecht, BI-TP 81/09 (1981). D. Schildknecht, BI-TP 81/12 (1981).

2.0 ELECTROWEAK INTERACTIONS OF THE CHARGED LEPTONS

The reactions

$e^+e^- \longrightarrow e^+e^-$ Bhabha Scattering

$e^+e^- \longrightarrow \mu^+\mu^-$ Muon Pair Production

$e^+e^- \longrightarrow \tau^+\tau^-$ Tau Pair Production

have been studied[9] at PETRA in terms of electroweak models. Although interference effects between the neutral weak boson and the photon mediated graphs could be measured in any of these interactions, the cleanest measurement of weak effects can be made in the foreward backward charge asymmetry in muon and tau pair production. Besides being sensitive to weak effects, these measurements are also uniquely sensitive to non-pointlike structure in the leptons since they are made at the highest available q^2.

For all of the measured processes, order α^3 QED calculations are necessary to test weak interaction effects because the order α^3 radiative corrections are generally about the same size as the weak effects. These calculations have been made by Berends, Gastmans, and Kleiss[10]. Monte Carlo event generators with the order α^3 matrix elements have been supplied to us by Berends and Kleiss. With these generators, we are able to pass the events through our detector simulation and analysis programs so that the effects of resolution and experimental cuts on the radiative corrections can be

---

[9] CELLO-Collaboration: H.J. Behrend et al., Phys. Lett. 103B (1981) 148, DESY Report 82-019 (1982), DESY Report 82-020 (1982). JADE Collaboration: W. Bartel et al., Phys. Lett. 88B (1979) 171, Phys. Lett. 92B (1980) 206 and Phys. Lett. 99B (1981) 281, Phys. Lett. 108B (1982) 140. MARK-J Collaboration: D. P. Barber et. al., Phys. Rev. Lett. 43 (1979) 1915, Phys. Lett. 95B (1980) 149, PHys. Rev. Lett. 48 (1982) 1701. PLUTO Collaboration: Ch. Berger et al., Zeitschr. f. Physik C1 (1979) 343, Zeitschr. f. Physik C7 (1981) 289, Phys. Lett. 99B (1981) 489. TASSO Collaboration: R. Brandelik et al., Phys. Lett. 92B (1980) 199, Phys. Lett. 94B (1980) 259, Phys. Lett. 110B (1982) 173, DESY Report 82-032 (1982).

[10] F. A. Berends, K. F. J. Gaemers and R. Gastmans, NP B63 (1973) 381. F. A. Berends, K. F. J. Gaemers and R. Gastmans, NP B68 (1974) 541. F. A. Berends and R. Kleiss, DESY-Report 80-66 (1980).

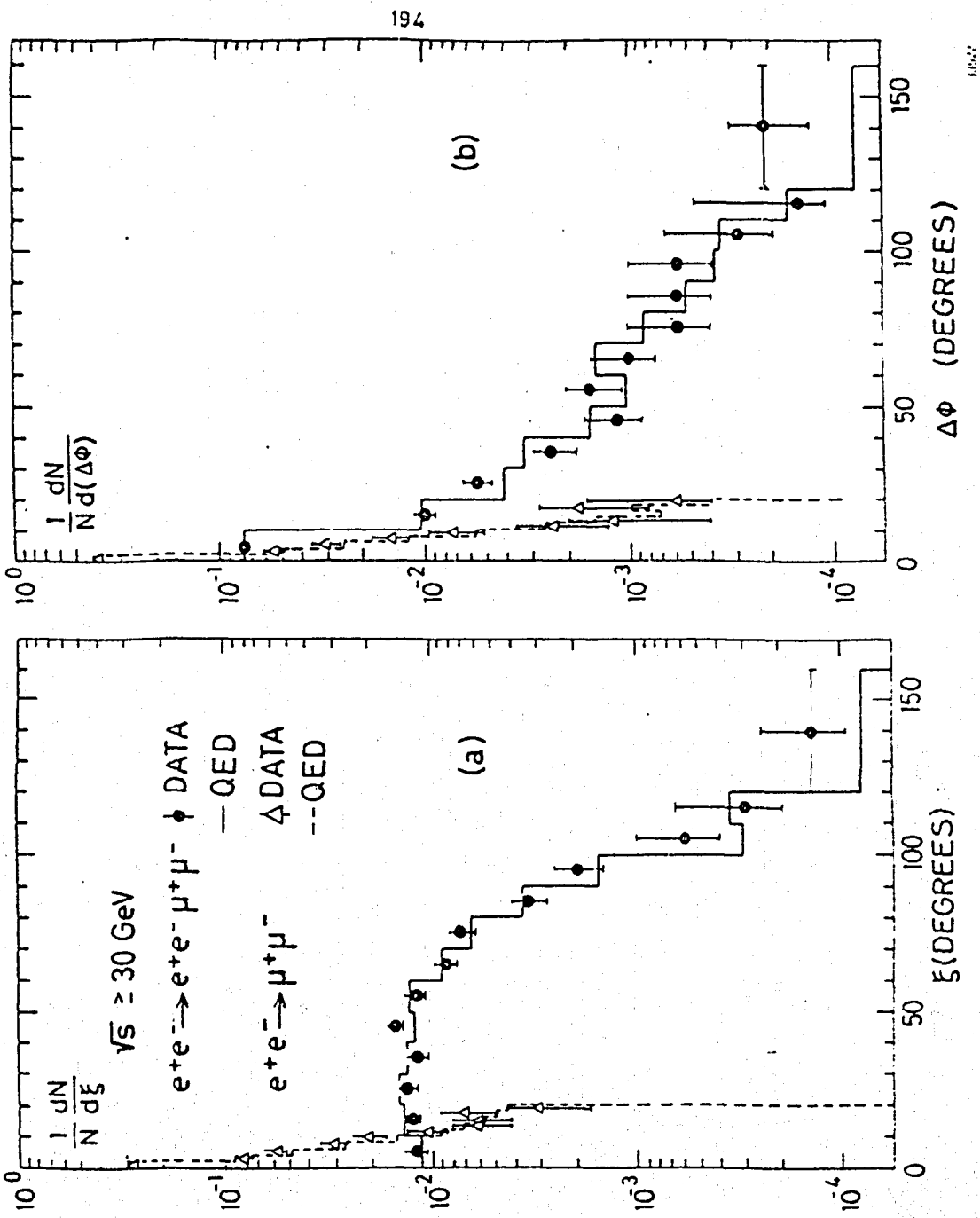

Figure 1. : Acollinearity and acoplanarity distributions for muon pair production.

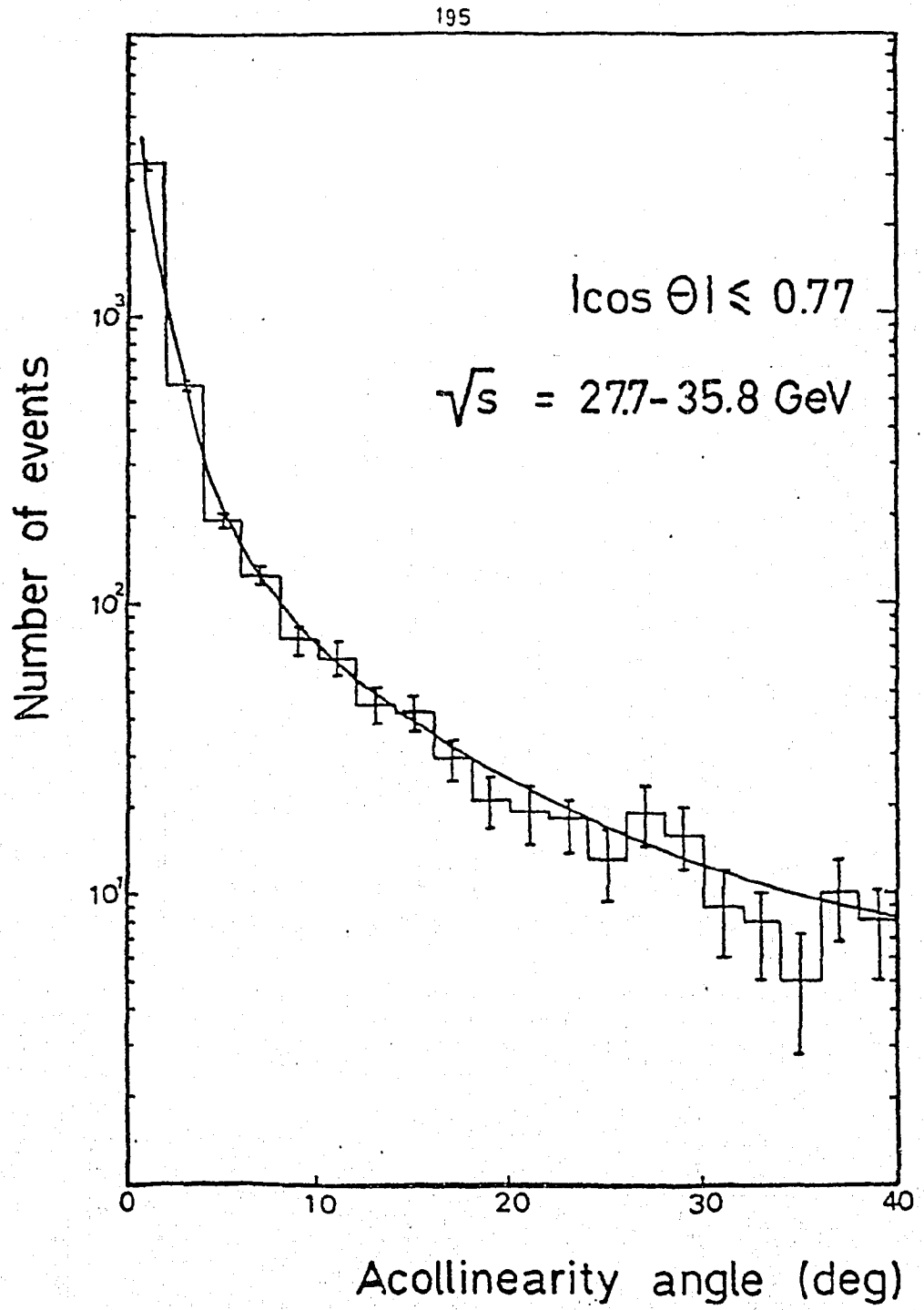

Figure 2. : Acollinearity distribution for Bhabha scattering.

accurately represented. Of particular note is the inclusion of hadronic vacuum polarization effects in a form slightly modified from that originally published by Berends and Komen[11]. Some effects of radiation of photons can be measured as a partial check of the calculations. In Figure 1 on page194 the measured acollinearity and acoplanarity distributions for muon pair production are compared to the expectation from Monte Carlo. Good agreement is found. Similarly, the acollinearity distribution for Bhabha scattering shown in Figure 2 on page195 agrees well with expectation.

2.1 BHABHA SCATTERING

The data from Bhabha scattering that are of relevance to our tests of the electroweak interaction are the angular distributions of the final state electron and positron. In the absence of beam polarization, the distribution is symmetric in the azimuthal angle Φ, but has a very strong dependence in the polar angle Θ from the beam axis.

Figure 3 on page 197 is a graph of $s(d\sigma/d\cos\Theta)$ for three center of mass energies. Data, with error bars invisible on this scale, are compared with the Monte Carlo calculation of order α^3 QED. As the cross section is steeply falling, it is difficult to see the details of the match between measurement and theory. A more clear exposition of this may be obtained by plotting the fractional difference between data and theory.

$$\delta = \frac{N_{DATA} - N_{QED}}{N_{QED}} \qquad (5)$$

In Figure 4 on page198 the distributions from Figure 3 on page197 are shown again as a graph of δ vs. $\cos\Theta$. If the data agreed exactly with QED, the points should lie on the horizontal line at 0. The solid line drawn in the figure is the expectation for the standard model of Glashow, Weinberg and Salam, with $\sin^2\Theta_w=0.23$. One can see in the plots of the data at lower energies that the expected difference between QED and GWS is smaller than at high energy. The data at high energy favor GWS over pure QED but are not conclusive. A 3% systematic point to point error is included in the error bars. At lower energies the data are equally compatibele with QED or QED plus weak interactions.

---

[11] F. A. Berends and G. J. Komen, Phys. Lett. 63B (1976) 432.

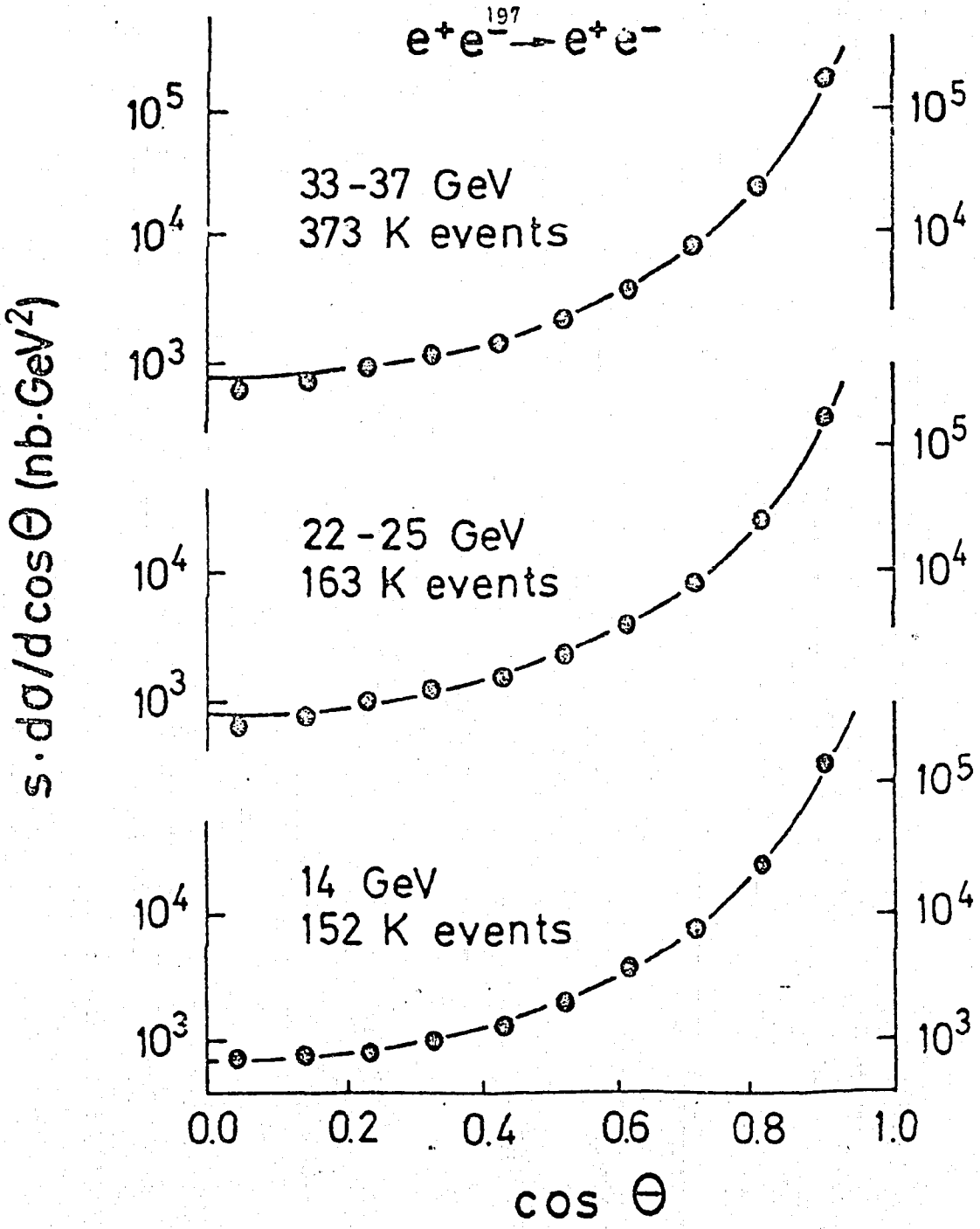

Figure 3. : Bhabha scattering angular distributions from MARK-J compared to pure QED.

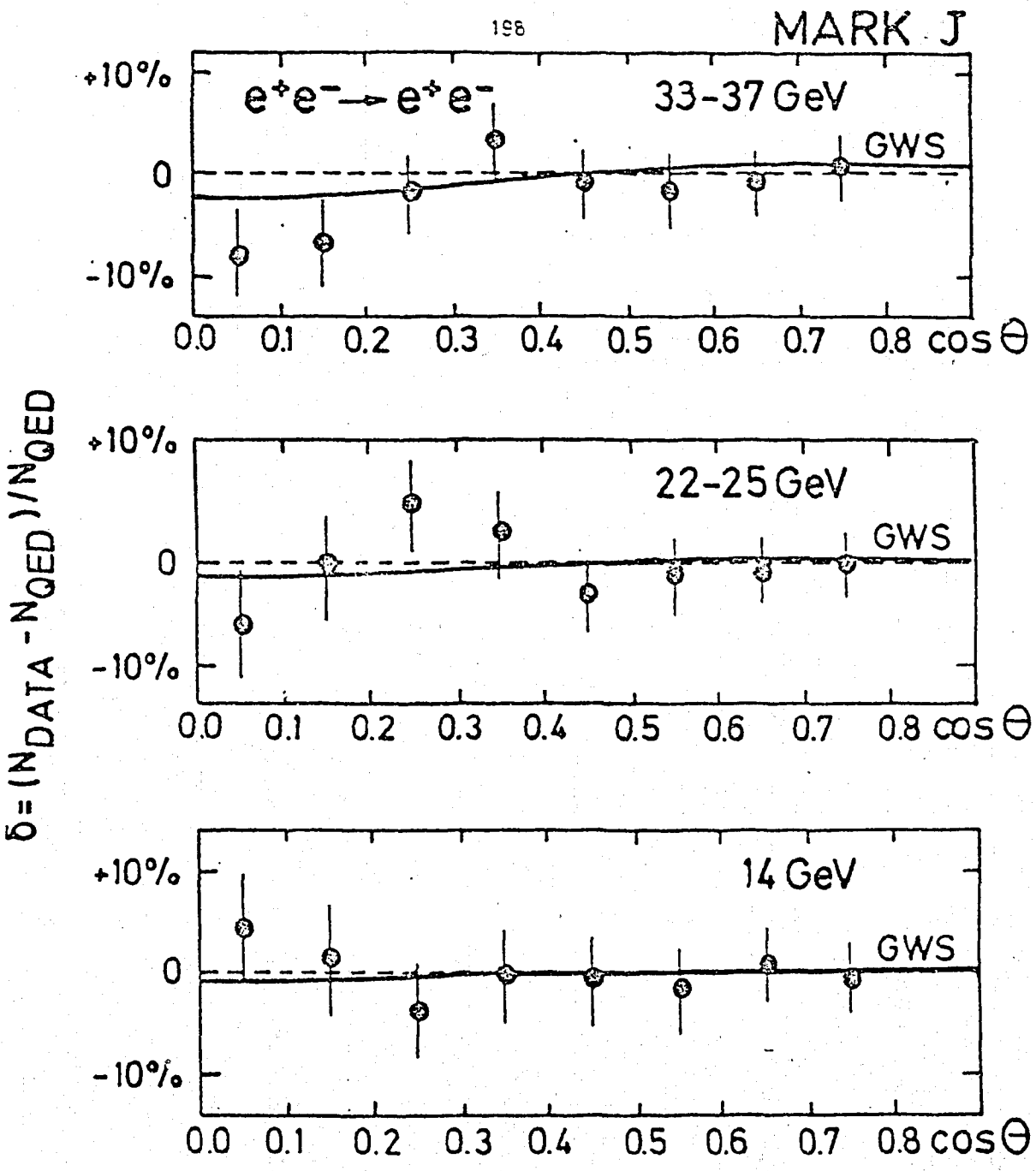

Figure 4. : The difference between data and QED is compared to the prediction of the GWS model with $\sin^2\theta_w=0.23$.

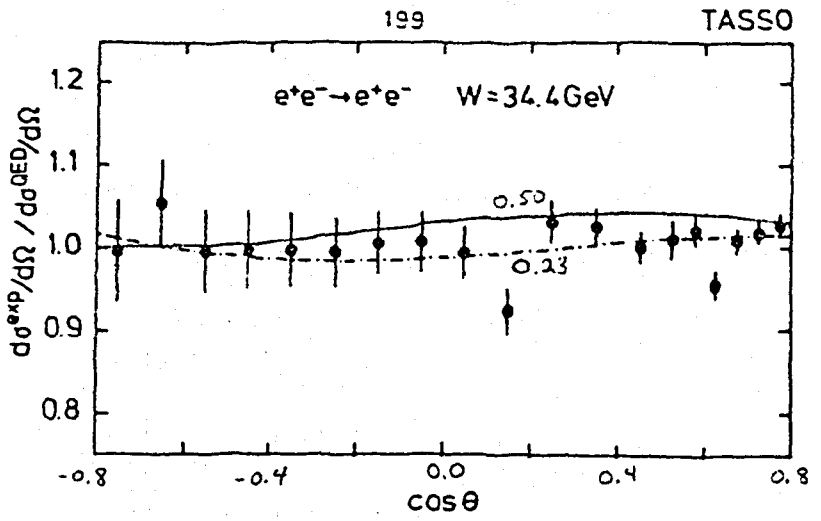

Figure 5. : TASSO data compared to electroweak predictions with different values of $\sin^2\Theta_w$.

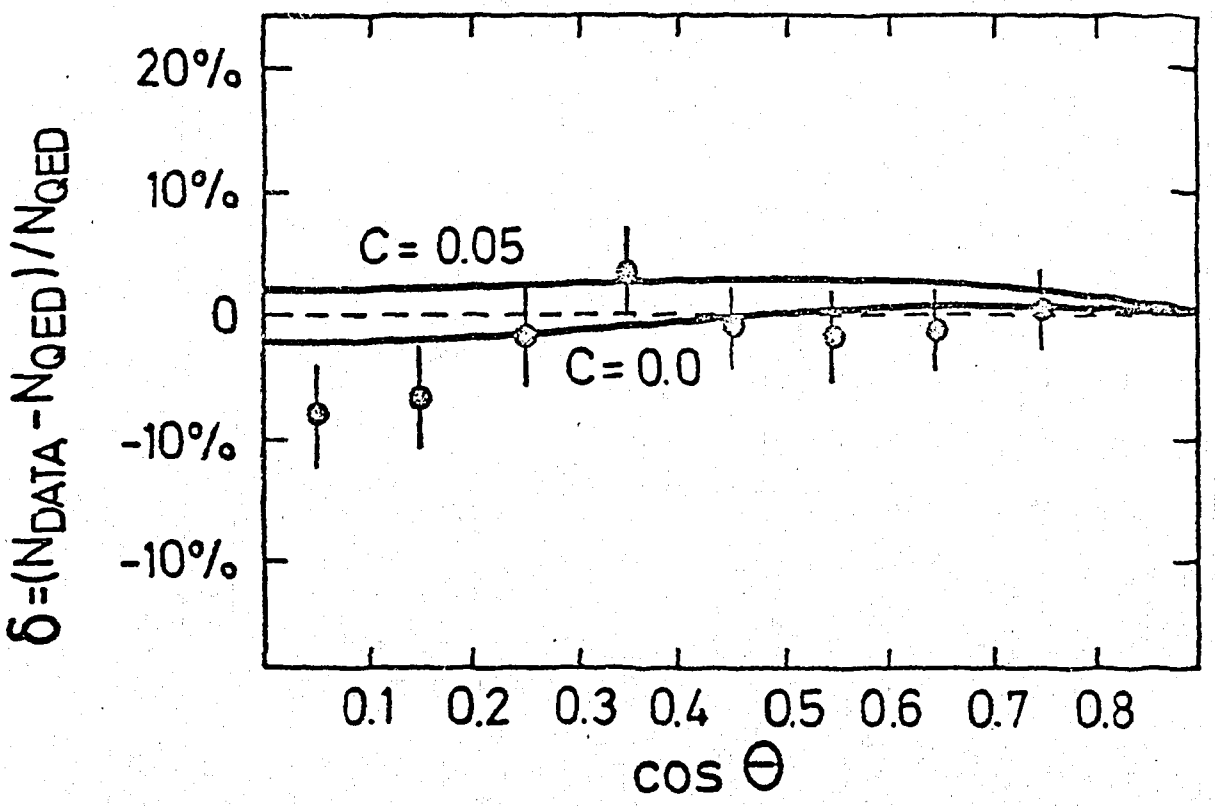

Figure 6. : MARK-J data compared to electroweak predictions with different values of C.

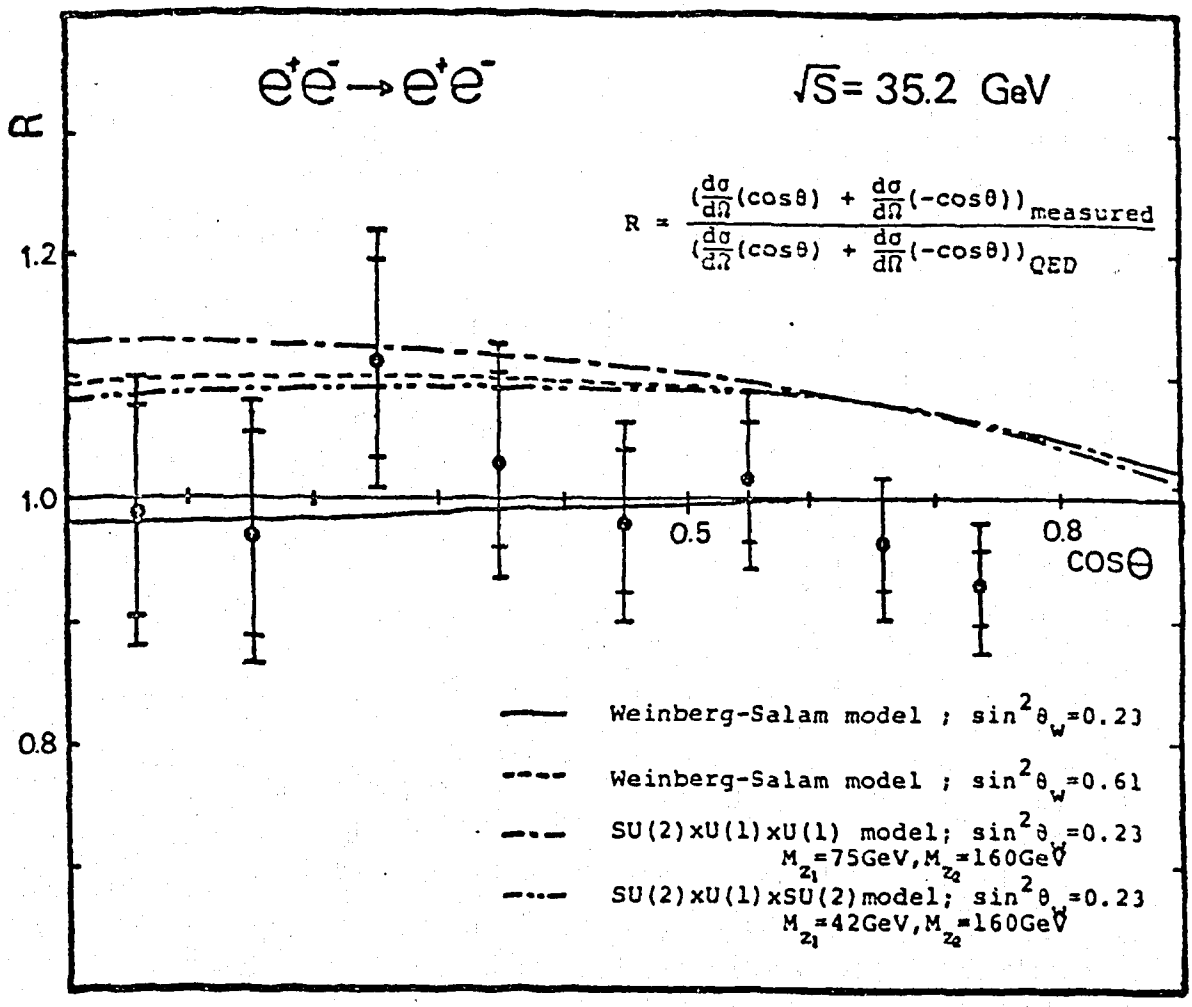

Figure 7. : JADE data compared to predictions for multiboson models.

Although the weak effects expected in the standard model are small, they may be much larger if we use other possible models. For example, Figure 5 on page199 shows the TASSO data compared to the standard model with different values of $\sin^2\Theta_w$. As you can see from the figure, the minimum effect is near the measured value of $\sin^2\Theta_w$. Figure 6 on page199 compares the MARK-J data to models with different values of C. C = 0 fits the data well, while C = 0.5 is obviously excluded because the line lies above almost all points. In Figure 7, δ from the JADE experiment is compared to electroweak models with multiple Z bosons.

2.2 MUON AND TAU PAIR PRODUCTION

In muon pair production, the total cross section and the polar angular distribution are sensitive to weak effects. The weak effect is expected to be small for the total cross section in the case of the standard model. However, like the results for Bhabha scattering, if one goes outside the standard model, the effects on the total cross section may be quite large. On the other hand, the weak effect in the angular distribution, and in particular, in the forward-backward charge asymmetry, is of measurable size in the standard model and generally larger in other models. We will, therefore look at both the total cross section and the forward-backward asymmetry, but will not be too surprised if it is the charge asymmetry where we can observe weak effects.

The radiative correction to $d\sigma/d\Omega$ for muon pair production is shown in Figure 8 on page202 as a function of the polar angle θ. This correction is for the particular cuts on muon pair events that each muon have at least 50% of a beam energy and that the two muons be collinear within 20°. The correction is not symmetric about 90°, indicating that there is a pure QED forward-backward charge asymmetry, which must be corrected for, to measure weak effects. I will discuss this correction again when I come to the charge asymmetry.

The data on the total muon pair production cross section are summarized in Figure 9 on page203. Results from all five PETRA experiments are shown as a function of $\sqrt{s}$. The data have been corrected for radiative effects and are, therefore, compared to the simple prediction of lowest order QED. Neither large disagreements nor unusual structure are found. Figure 10 on page204 is similar to Figure 9 on page203 but the tau pair production cross section is plotted rather than that for muons. Again, no unusual structure is seen.

The angular distributions from the individual experiments are shown in Figure 11 on page205. A foreward backward charge asymmetry is already apparent in these distributions. In Figure 12 on page205, the tau pair angular distribution from the CELLO group is shown.

2.3 CHARGE ASYMMETRY

The final item of data on the electroweak interaction of the charged leptons is the forward-backward charge asymmetry in the production of muon pairs and of tau pairs. The polar angle θ is defined as the angle between the initial electron direction and the final μ^- or τ^- direction. The forward hemisphere is then defined as $0° < \theta < 90°$ and the backward hem-

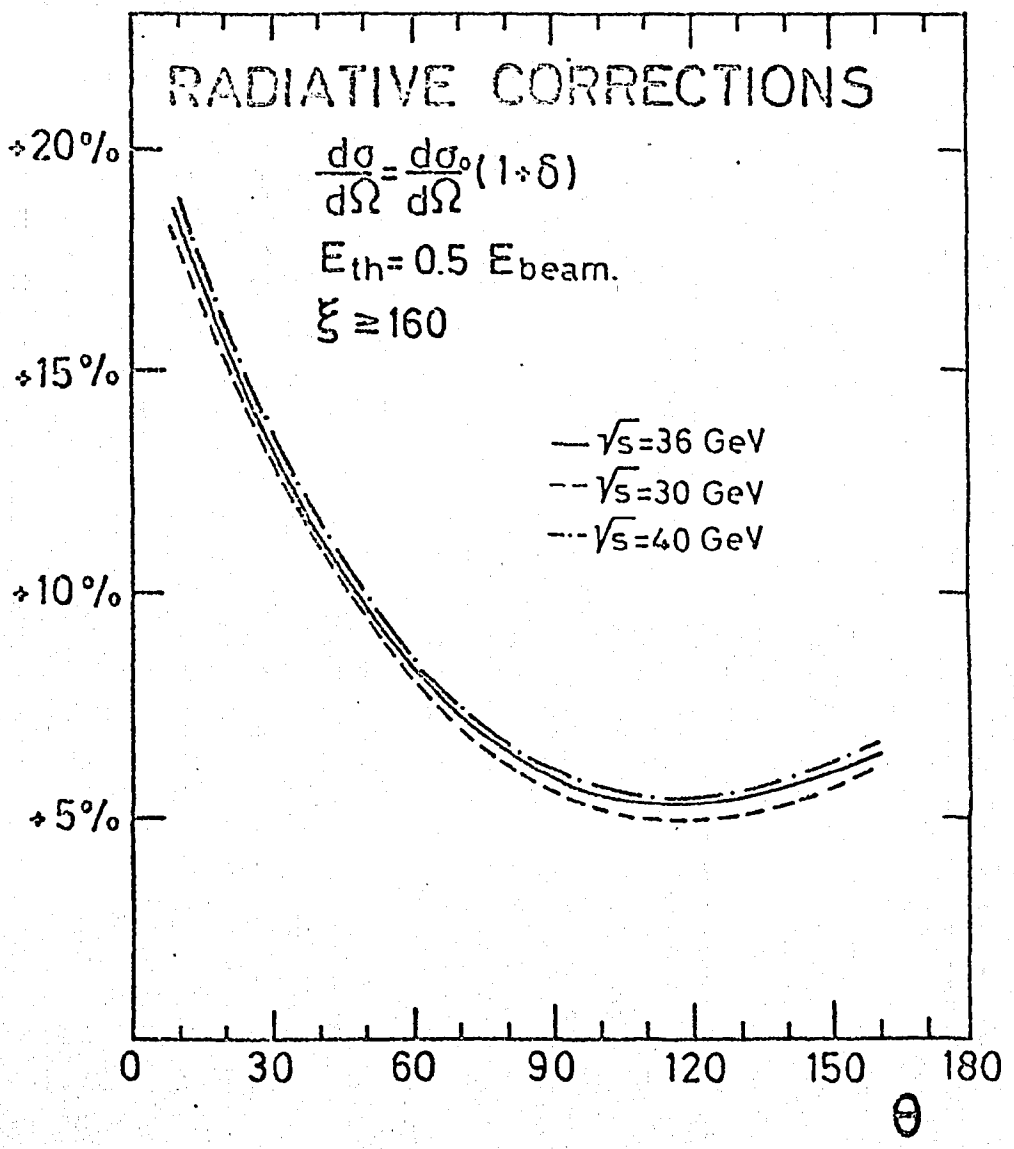

Figure 8. : Radiative correction to muon pair production as a funtion of polar angle.

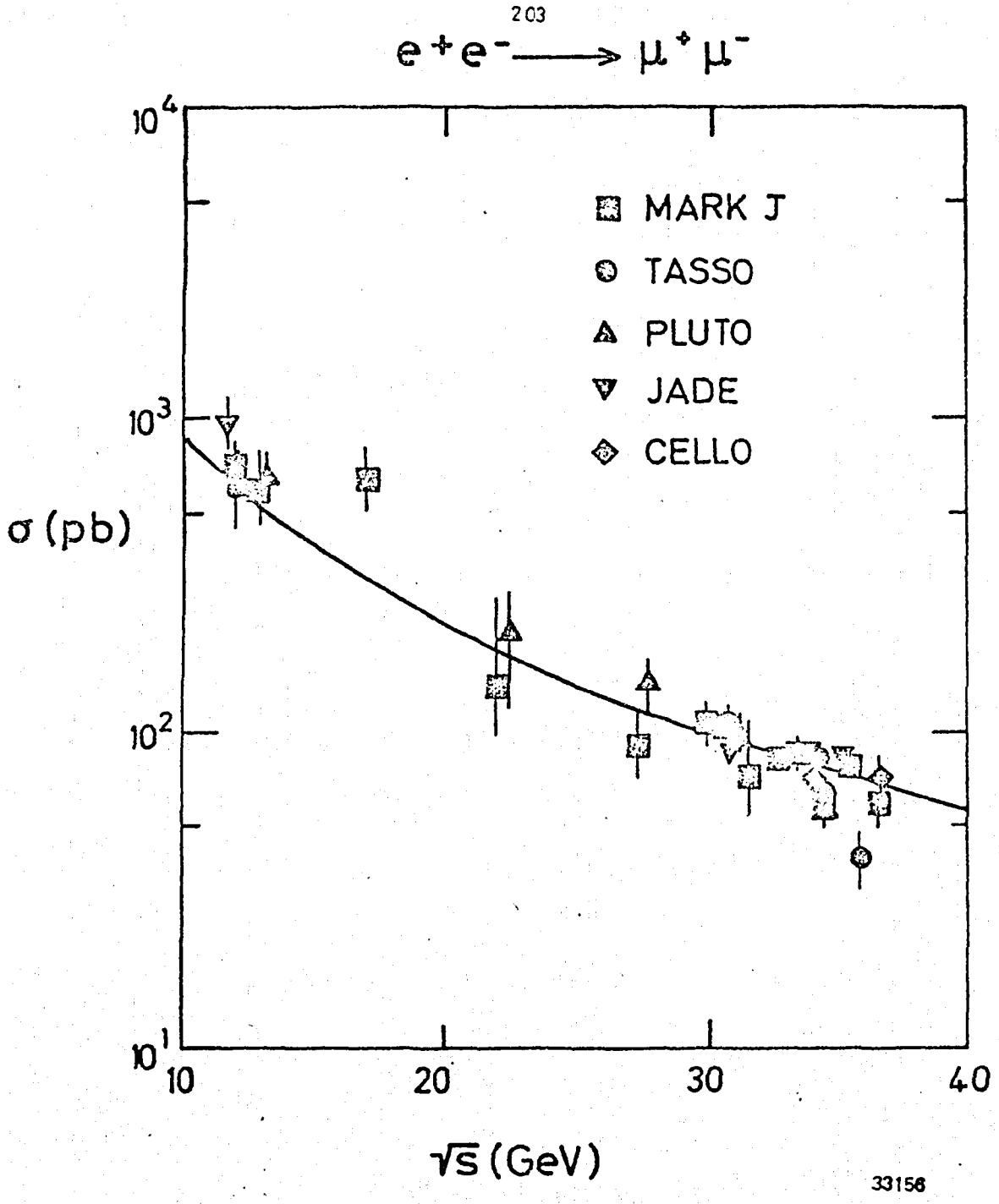

Figure 9. : Total muon pair production cross section vs. $\sqrt{s}$.

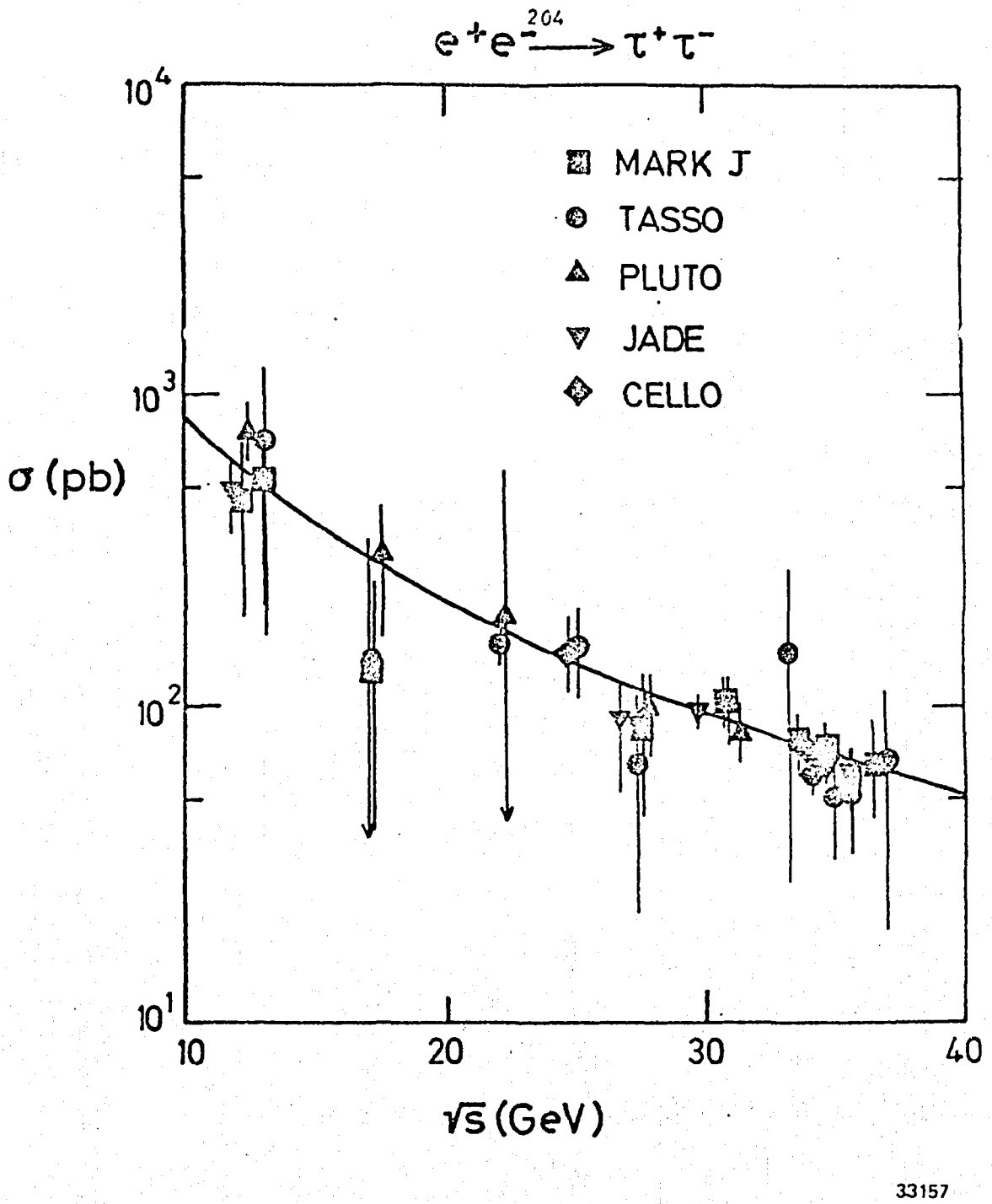

Figure 10. : Total tau pair production cross section vs $\sqrt{s}$.

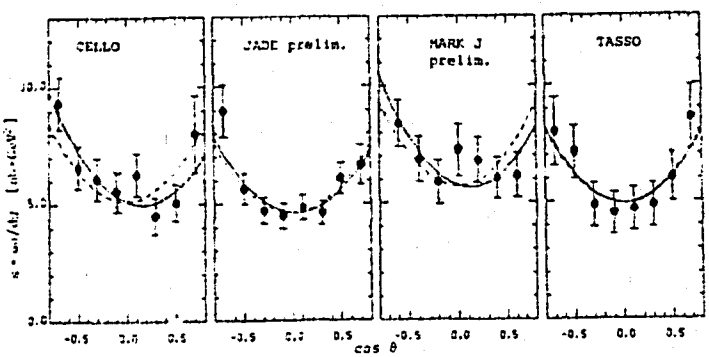

Figure 11. : Angular distribution for muon pair production from four groups.

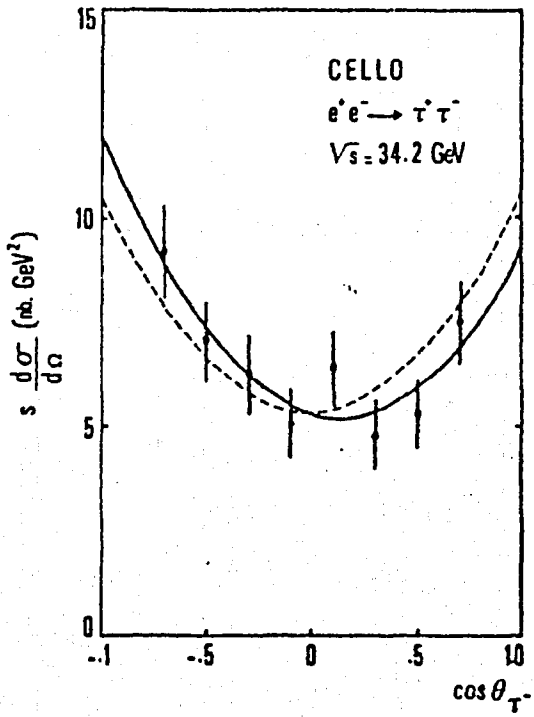

Figure 12. : Angular distribution for tau pair production from CELLO.

isphere as $90° < \Theta < 180°$. The asymmetry as a function of Θ is defined to be

$$A_{\mu\mu}(\Theta) = \frac{N_{\mu^-}(\Theta) - N_{\mu^-}(\pi-\Theta)}{N_{\mu^-}(\Theta) + N_{\mu^-}(\pi-\Theta)} \quad . \tag{6}$$

Since statistics are still low, the number usually quoted is integrated over angle

$$A_{\mu\mu} = \frac{N_{FOREWARD} - N_{BACKWARD}}{N_{FOREWARD} + N_{BACKWARD}} \quad . \tag{7}$$

Experimentally, an asymmetry of this sort is a particularly easy thing to measure accurately. To make a systematic error, the detector must have an unexpected difference in acceptance between high momentum μ^+'s and μ^-'s. Since the only differences must be due to the small muon track curvature in the magnetic field, one would expect these effects to be small. No absolute knowledge of acceptance or luminosity is needed.

We can compute the asymmetry in lowest order using just the two diagrams

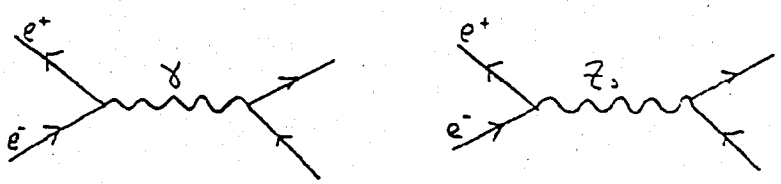

Using this lowest order computation, the differential muon pair cross section is

$$d\sigma/d\Omega = \alpha^2/4s\ [F_1(1+\cos^2\Theta) + F_2\cos\Theta] \qquad (8)$$

where

$$F_1 = 1 + 8sgg_V^2\left(\frac{M_z^2}{s-M_z^2}\right) + 16s^2g^2(g_A^2+g_V^2)^2\left(\frac{M_z^2}{s-M_z^2}\right)^2$$

$$F_2 = 16sgg_A^2\left(\frac{M_z^2}{s-M_z^2}\right) + 128s^2g^2g_A^2g_V^2\left(\frac{M_z^2}{s-M_z^2}\right)^2$$

$$g = G_F/8\sqrt{s}\pi\alpha = 4.49\cdot10^{-5}\ GeV^{-2}$$

and g_A amd g_V are the previously defined axial vector and vector coupling constants for the charged leptons.
The asymmetric piece of the cross section is the part proportional to cos Θ. By putting in some numbers one can see that at PETRA, energies F_2 is small compared to F_1 and that, in both F_1 and F_2, the first terms dominate. The first term in F_1 is the purely electromagnetic term and the first term in F_2 is due to weak electromagnetic interference. We may then write down an approximate formula for the asymmetry to investigate its dependence on the lepton coupling constants, the mass of the Z_0, the center of mass energy and the polar angle.

$$A_{\mu\mu} \approx 7\cdot10^{-4}\ s\ g_A^2\left(\frac{M_z^2}{s-M_z^2}\right)\frac{\cos\Theta}{1+\cos^2\Theta} \qquad (9)$$

This formula is graphed in Figure 13 on page208.

The asymmetry in this approximation depends only on the axial vector coupling of the electron and muon. It grows as the center of mass energy squared for $s << M_z^2$ and is negative in this region. As s approaches M_z^2, the pure weak terms of course must also be included. Since the effect grows sharply with $\sqrt{s}$, it is important to make measurements at as high an energy as possible. From the figure we can see that by running at 40 GeV, we get nearly twice the asymmetry as running at 30 GeV. Finally, the simple angular dependence of the asymmetry is plotted in the figure and

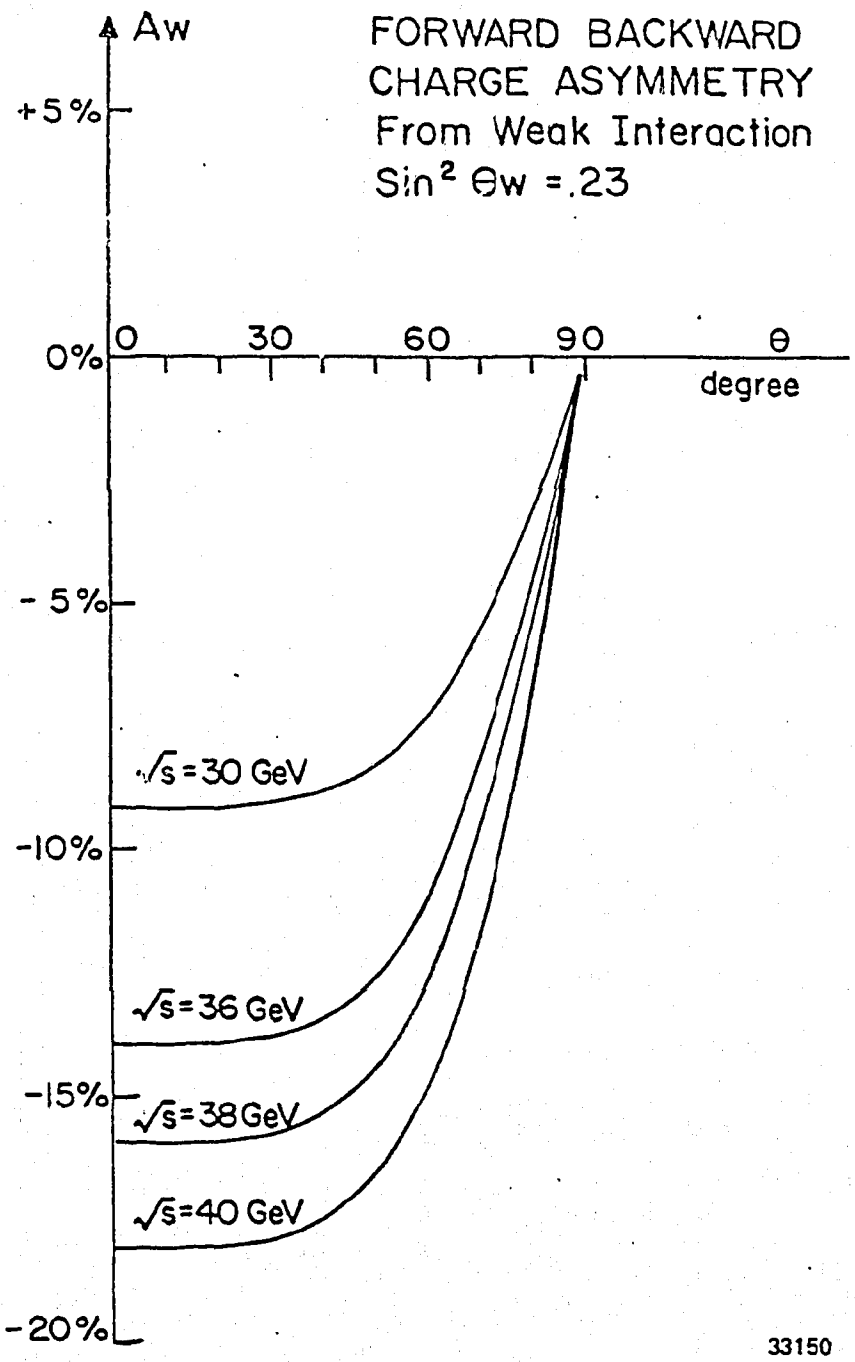

Figure 13. : Expected asymmetry vs. θ.

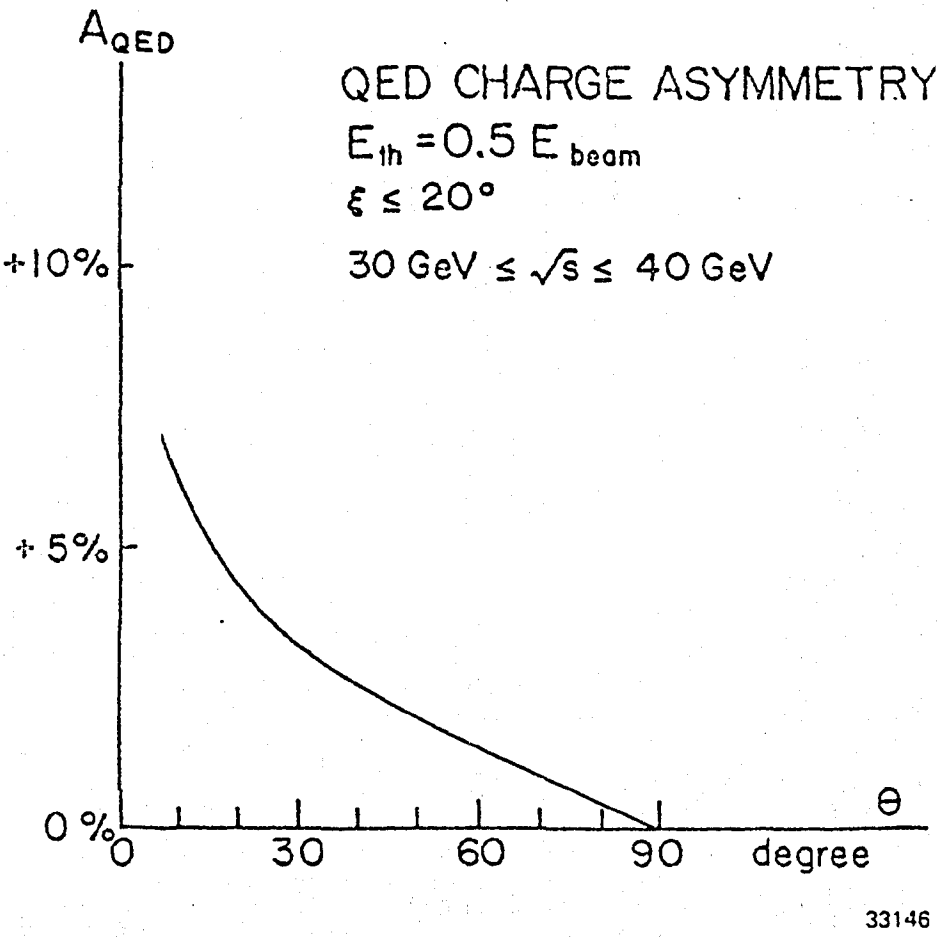

Figure 14. : Asymmetry due tc QED vs. θ.

it should be noted that the maximum effect is at small angle to the beam. So it is important to measure over a large acceptance to get the maximum effect.

Of course to do the calculation properly, we must look at order α^3 effects from QED. These are included in the Monte Carlo generator and the QED asymmetry due to them is shown in Figure 14 on page209. This asymmetry is somewhat smaller than that we expect from weak effects, but is of opposite sign. It gets large as $\theta \to 0$ but the experiments do not measure for $|\cos\theta| > 0.8$ so that the maximum effect is around 3% and the angular averaged effect is about 1.5%. This indicates that higher order QED effects may be neglected. The data from each experiment are corrected for this pure QED radiative effect. In addition to the pure QED correction to the expected asymmetry, there is a radiative correction to diagrams containing a Z_0 which will of course depend on the particular weak interaction model. One obvious effect is a reduction of the magnitude of an expected asymmetry due to the effective lowering of s by hard initial state photon emission. We use a Monte Carlo[12] to calulate the expected asymmetry and find that it is reduced by 0.8% from the simple calculation.
Since this is model dependent, we do not correct the data for this but rather quote a corrected value of the expected asymmetry from the GWS model.

Significant measurements of the charge asymmetry have been presented by four experiments at PETRA. All of these groups estimate that their systematic error in determining the charge asymmetry is very small, that is, approximately 1%. The experiments have made studies of their systematic errors on the charge asymmetry. Each experiment finds that the probability of double charge confusion is very small by comparing the number of μ pairs measured to have like charge to the number measured to have opposite charge. As an example, the data from MARK-J are shown in Figure 15 on page211. Here the signed momentum of one muon is plotted vs. that for the other. One can see directly that the probability for charge confusion is small. Typically, the fraction of like charge is about 1% implying a very small amount of double charge confusion. Asymmetric backgrounds such as cosmic rays or e^+e^- production have been shown to be very small.

To determine whether the detector has a charge asymmetric acceptance, TASSO has studied the charge asymmetry in hadron production and found it to be very small. In order to more closely duplicate the topology and curvature of the μ pairs, JADE and MARK-J have measured the detector

---

[12] F. Berends, R. Kleiss and S. Jadach, private comunication.

asymmetry using high momentum cosmic rays and each has found it to be $\lesssim$ 1%. Figure 16 on page 212 shows the MARK-J measurement of the detector asymmetry binned in cos Θ.

In addition, MARK-J has the ability to change the polarity of its magnetic field at regular intervals during data taking without affecting the beams. A positive muon, bending under one polarity magnetic field, is identical in the detector to a negative muon bending under the opposite polarity. Therefore, by taking equal amounts of data at each polarity, MARK-J can cancel any detector asymmetry. This is particularly true since the polarity is changed often to assure cancelation of any time dependent effects.

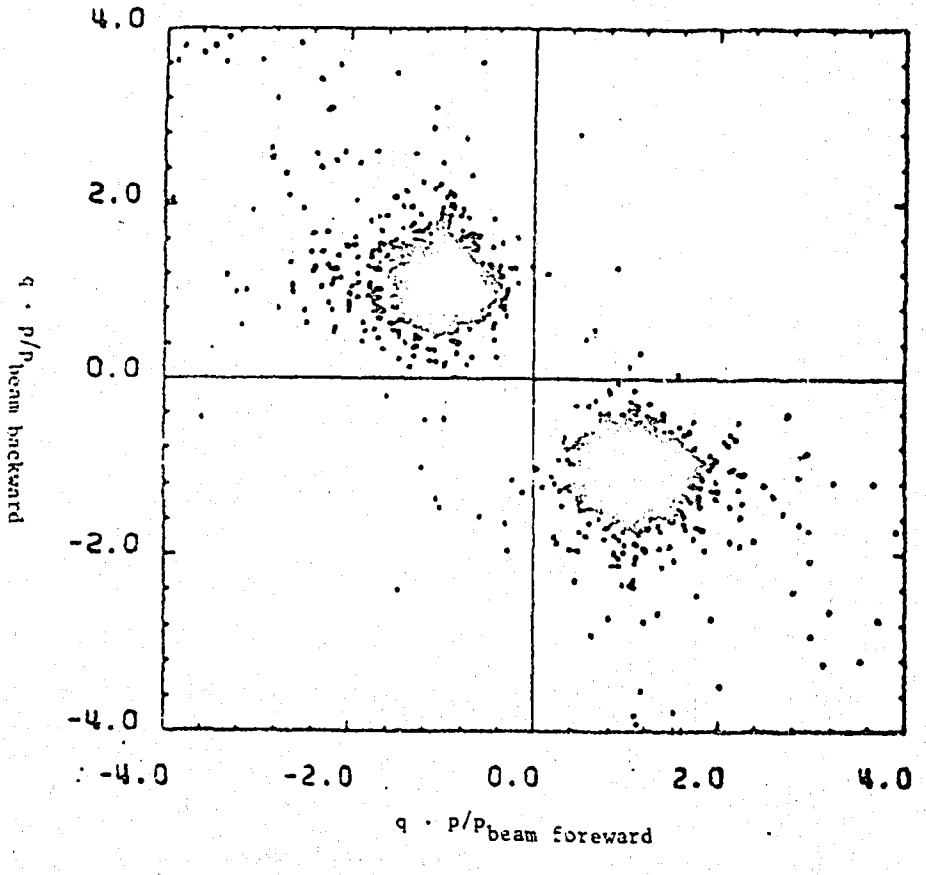

Figure 15. : Charge * momentum for foreward muon vs. charge * momentum for backward muon.

The measured asymmetries are given in Table I. A fit is made to the values of F_1 and F_2 as in equation (8). The asymmetry extrapolated to 4π solid angle coverage is $3F_2/8F_1$. This number is quoted to facilitate averaging of experiments and as a number which can be compared to new theories, since it does not depend on the details of the detector. Values for the tau pair asymmetry are also given but are obviously of less statistical relevance. The average center of mass energy is around 34 GeV.

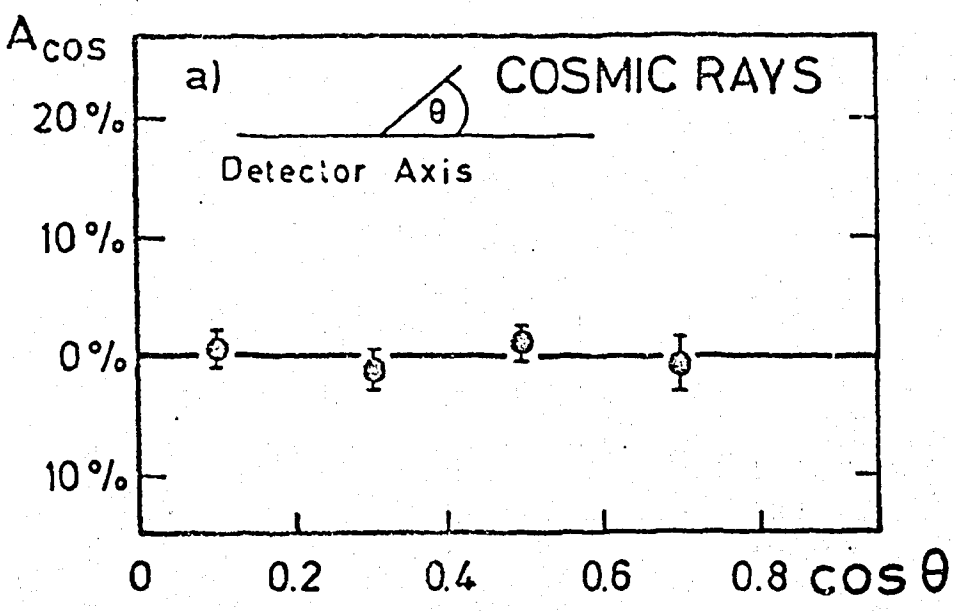

Figure 16. : Asymmetry measured for high momentum cosmic rays vs. cos(θ).

TABLE I

MEASURED VALUES OF ASYMMETRIES

GROUP	$A_{\mu\mu}$	$A_{\tau\tau}$
CELLO	- 6.4±6.4	-10.6±5.4
JADE	-12.7±2.7	- 5.9±5.3
MARK-J	- 9.8±2.3	- 7.0±7.2
TASSO	-16.1±3.2	- 0.4±6.9
COMBINED	-11.9±1.6	- 5.8±2.8
EXPECTED	- 8.7±0.6	- 8.7±0.6

The average value is of particular interest. Since the systematic errors are small, compared even to the combined statistical error, averaging greatly improves the precision of the measurement. A systematic error of 1% on each measurement has been included. The four data points give a χ^2 of 3.1 for three degrees of freedom.

The result, as shown in the table, is $A = -11.9\% \pm 1.6\%$ expecting -8.7% in the standard model. Thus weak effects have been observed at PETRA in this seven standard deviation effect. This is also the highest q^2 at which weak effects have been measured, the average q^2 being around 1200 GeV^2.

From the measurement, we can determine the axial vector coupling constant for the charged leptons assuming only universality and that we are far from Z_0 pole(s)

$$0.50 < |g_A| < 0.66$$

at the 95% confidence level. At large enough q^2, the asymmetry depends upon the Z_0 mass due to the propogator term $(M_z^2/s-M_z^2)$. At the present value of q^2, this contributes 1.5% to the asymmetry if $M\sigma_z$=90 GeV. We can therefore place limits on the Z_0 mass which do not depend on the GWS model. The only assumptions needed are that there is a single Z_0 and that $g_A=\pm0.5$ for electrons and muons as is expected in any model with the now well established SU(2) symmetry. We find at the 95% confidence level

$49\ \text{GeV} < M_z < 95\ \text{GeV}.$

2.4 INTERPRETATION OF LEPTONIC DATA

The simplest interpretation of the data is a measurement of $\sin^2\Theta_w$ in the standard model. Table II gives the results from the five PETRA experiments for $\sin^2\Theta_w$ determined from purely leptonic processes.

TABLE II

$\sin^2\Theta_w$ FROM PURELY LEPTONIC REACTIONS

CELLO	0.22±0.12
JADE	0.25±0.15
MARK-J	0.25±0.11
PLUTO	0.23±0.17
TASSO	0.25±0.10

The value of 0.25 for $\sin^2\Theta_w$ is a very likely one because this type of experiment is sensitive to g_A^2 and to g_V^2. If the effect of g_V^2 is measured to be less than zero, then the best that can be done within the standard model is to make $g_V^2 = 0$, in which case $\sin^2\Theta_w=0.25$. On the other hand, if g_V^2 is measured to be greater than zero, this can be produced by two values of $\sin^2\Theta_w$ symmetric about 0.25. This means that the central value is likely to be near to 0.25 unless g_V^2 is actually limitted to be greater than zero in which case the two solutions separate. Since g_V is indeed expected to be very small compared to the accuracy with which it is measured here, the experiments have a very good chance of measuring $\sin^2\Theta_w=0.25$. Note, however, that because M_z^2 depends on $\sin^2\Theta_w$ in the standard model, values other than $\sin^2\Theta_w=0.25$ can give the best fit, even if $g_V^2 \leq 0$, due primarily to propagator effects in the asymmetry.

It should be pointed out again that no disagreement with the standard model has been found. So our result, in terms of the standard model, is that $\sin^2\Theta_w=0.25\pm0.10$.

Outside the standard model, we may determine g_A and g_V for charged leptons. This will also show quantitatively whether the data are in agree-

ment with the standard model. Figure 17 on page215 shows the measured value of g_A^2 versus the measured value of g_V^2 for five PETRA experiments with error bars denoting the one sigma error. The points cluster together quite well in a region near $g_V^2 \approx 0.0$ and $g_A^2 \approx 0.2$. Because we look at g_V^2, the prediction is symmetric about $\sin^2\Theta_w=0.25$ which explains the double labelling of the axis. For $\sin^2\Theta_w=0.25$, g_V^2 is zero. The model predicts $g_A^2=0.25$ independent of $\sin^2\Theta_w$. Most of the data points are within one sigma of the standard model with $\sin^2\Theta_w=0.23$ as measured in neutrino scattering from hadrons.

Alternatively, we may compare and combine our results with those of another purely leptonic process, neutrino electron scattering. In Figure 18 on page216 , the results of determination of g_A and g_V for the charged leptons are shown for ν-e scattering and for the MARK-J data from PETRA. The ν-e scattering 68% confidence level limits are the three elliptical regions. By combining three different kinds of experiments, the coupling constants can be limited to two regions in the plane. These are the dark regions in the figure at the overlap of all three elliptical regions. We can discriminate between the two regions by using the data from MARK-J. The shaded area centered at the origin is the 95% confidence level contour from the e^+e^- data. This area is symmetric about the lines $g_A=0$ and $g_V=0$ because only g_A^2 and g_V^2 have any significant effect on the e^+e^- data. These data nicely eliminate one of the two solutions, leaving only the one near $g_A=0.5$ and $g_V=0.2$. So combining all of the data, one can limit g_A and g_V to be a small region which again is quite consistent with the standard model shown by the line. These data, however, are from different q^2 regions, the ν-e data coming from very low q^2 and the e^+e^- data from $q^2 \sim 0.15 \cdot M_Z^2$.

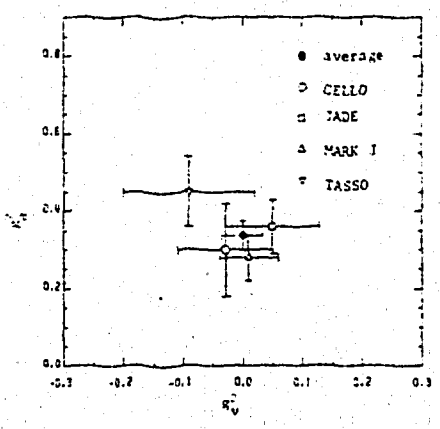

Figure 17. : Measured values g_A^2 and g_V^2.

ELECTROWEAK INTERACTIONS OF THE CHARGED LEPTONS

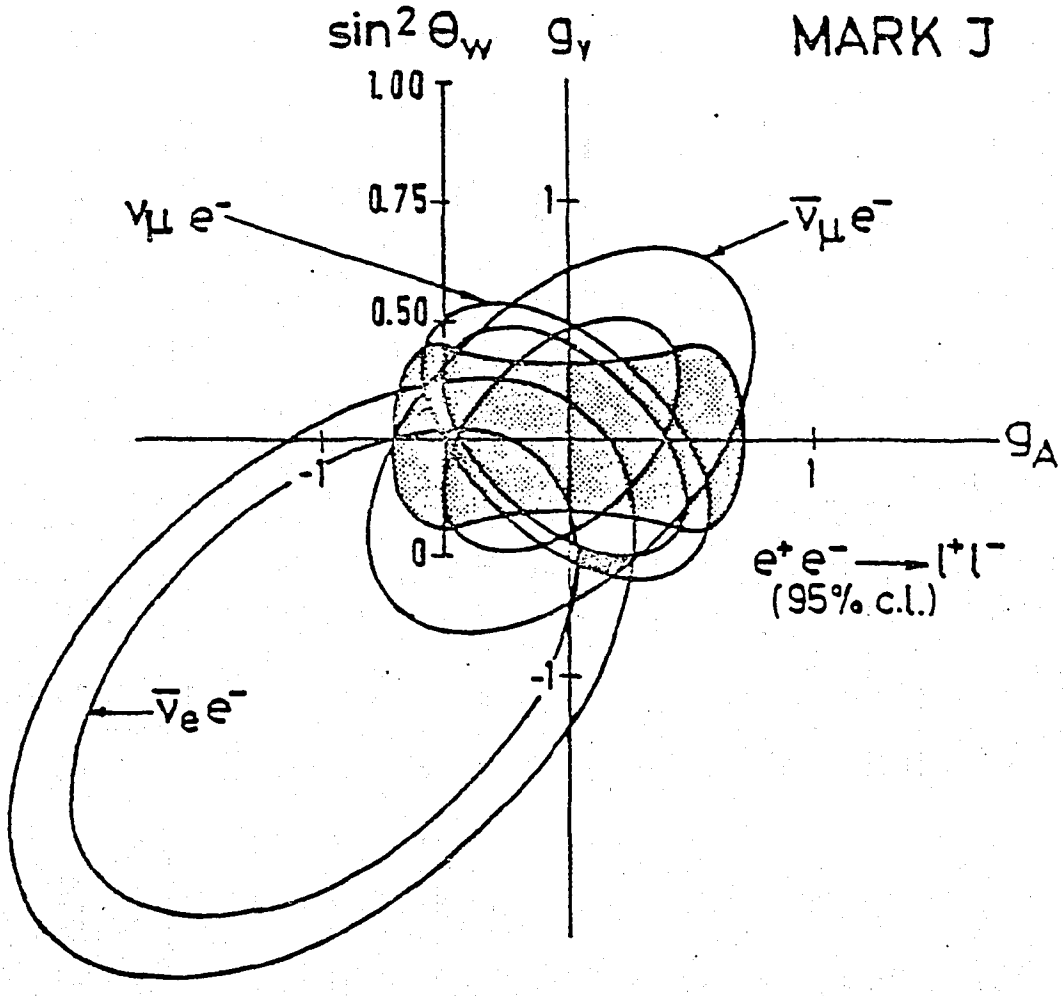

Figure 18. : Allowed regions in the g_A - g_V plane from three electon scattering experiments (68% CL ellipses) and from MARK-J (shaded area).

In the introduction, I defined the parameter C, which is the coefficient of a term in the weak neutral current Hamiltonian proportional to the electromagnetic current squared. This kind of term is expected in multiboson weak models and also in more radical models where there is a continuum of weak interactions perhaps due to a constituent nature of the weak bosons. With multiple bosons, the model can no longer be parameterized in terms of g_A and g_V only. C is expected to be greater or equal to zero in all models.

Limits on C, which are applicable to any model of the weak neutral current, have been obtained by all of the PETRA experiments and are shown in Table III. All the results are consistent with C = 0.

TABLE III

95% CONFIDENCE UPPER LIMITS ON C

CELLO	0.032
JADE	0.039
MARK-J	0.027
PLUTO	0.060
TASSO	0.030

If we take the tightest of these limits, we may put a limit on the normalized difference between the actual theory and the standard model, which is equal to 16 C. More specifically,

$$\frac{\left[\int ds\ s\cdot\sigma(e^+e^-\to ALL)\right]_{ACTUAL} - \left[\int ds\ s\cdot\sigma(e^+e^-\to ALL)\right]_{GWS}}{\left[\int ds\ s\cdot\sigma(e^+e^-\to ALL)\right]_{GWS}} < 0.43$$

at the 95% confidence level. Therefore, in terms of this weighted integral over all energy, we have determined that the actual theory of weak interactions is within 50% of the standard model.

As examples, we have looked at two specific[7] models of simple extensions of the standard model. These are

$$SU(2) \times U(1) \times U(1)$$

and

$$SU(2) \times U(1) \times SU(2).$$

They add more weak bosons but leave all of the low energy predictions of the standard model unchanged. These models have two new parameters added to the single parameter of the standard model, $\sin^2\Theta_w$. These two parameters can be chosen to be M_1 and M_2, the masses of the two neutral bosons in the model. The coupling strength of the two bosons will depend on M_1 and M_2. C can then be expressed in terms of the model parameters.

In SU(2)×U(1)×U(1)

$$C = \cos^4(\Theta_W)\ (M_z^2/M_1^2 - 1)\ (1 - M_z^2/M_2^2) \qquad (10)$$

and in SU(2)×U(1)×SU(2)

$$C = \sin^4(\Theta_W)\ (M_z^2/M_1^2 - 1)\ (1 - M_z^2/M_2^2) \qquad (11)$$

Figure 19 on page219 shows the limits placed by our measurement on the parameter space for these two models. For SU(2)×U(1)×U(1), the 95% confidence level limit requires that one of the two Z's has a mass very close to the standard M_z. The other may have a very large mass or may actually have a small mass, in which case, one finds that its coupling strength becomes very small. For SU(2)×U(1)×SU(2), the constraint is not as tight, but about half of the parmeter space has been eliminated.

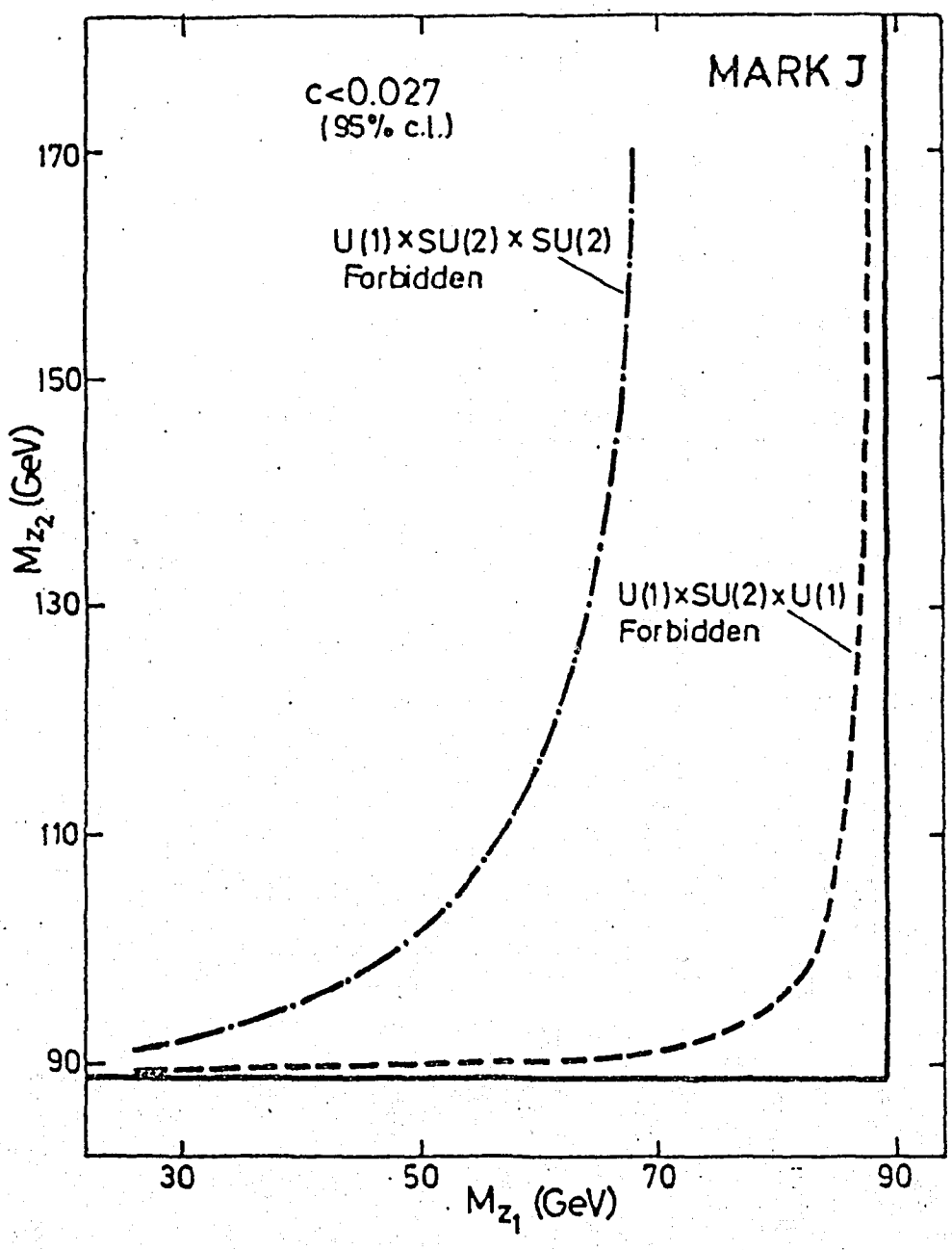

Figure 19. : Allowed regions in the M_1 - M_2 plane for two multiboson models.

3.0 ELECTROWEAK REACTIONS OF QUARKS

3.1 DETERMINATION OF THE WEINBERG ANGLE.

The data in e^+e^- on production of hadrons can also be used to test the electroweak interaction. In particular, the total hadronic cross section is sensitive to weak effects. The ratio of the total hadronic cross section, corrected for QED radiative effects, to the lowest order QED cross section for the production of muon pairs is known as R. R is just the sum over flavors and colors of R for each quark species.

$$R = \sum_{\substack{\text{flavors}\\ \text{colors}}} R_q \qquad (12)$$

To lowest order, R_q is

$$R_q = Q_q^2 - 8sgQ_q g_{Ve} g_{Vq}\left(\frac{M_z^2}{s-M_z^2}\right) + 16s^2g^2(g_{Ve}^2 + g_{Ae}^2)(g_{Vq}^2 + g_{Aq}^2)\left(\frac{M_z^2}{s-M_z^2}\right)^2 \qquad (13)$$

where $g_{Aq}=\pm 0.5$ and g_{Vq} is, in the standard model, approximately 0.19 for a charge 2/3 quark and -0.35 for charge 1/3. This is in contrast to the charged leptons, where $g_V \approx -0.08$. Weak effects in quark production have been calculated[13].
Of course there is also a well known QCD correction[14] to R.

$$R_q \rightarrow R_q(1 + \alpha_s/\pi + \ldots)$$

This correction is taken account of in the analysis but the results are insensitive to the value of α_s.

In Figure 20 on page221, measurements of R from MARK-J, at a wide range of center of mass energies, are compared to the predictions for different

---

[13] R. Budny, Phys. Lett. 55B (1975) 227. J. Ellis and M. K. Gaillard, "Physics with Very High Energy $e^+ e^-$ Colliding Beams", CERN 76-18 (1976) 21.

[14] K.G. Chetyrkin et al., Phys. Lett. 85B (1979) 277. M. Dine and J. Sapierstein, Phys. Lett. 42 (1979) 668. W. Celmaster and R. Gonsalves, Phys. Lett. 44 (1980) 560.

values of $\sin^2\theta_w$. The data agree well with the best fit for values of $\sin^2\theta_w$ of 0.29 but clearly disagree with the other values of $\sin^2\theta_w$ shown. Even though the systematic error on the measurement of R is large, the point to point error is estimated to be quite small, so that by measuring the energy dependence of R, we can make a good determination of weak effects[15] to R. PETRA has recently run at center of mass energies of 14 and 22 GeV, yielding high statistics measurements of R at those energies. From these data, along with the data on leptons from the previous section, we get a preliminary value from MARK-J of

$$\sin^2\theta_w = 0.27^{+0.08}_{-0.04}$$

This is now a very accurate determination of $\sin^2\theta_w$ at high q^2, $q^2 \sim 1300$ GeV^2. Using a similar analysis, JADE has obtained[16] a value from their combined data of $\sin^2\theta_w = 0.22 \pm 0.08$.

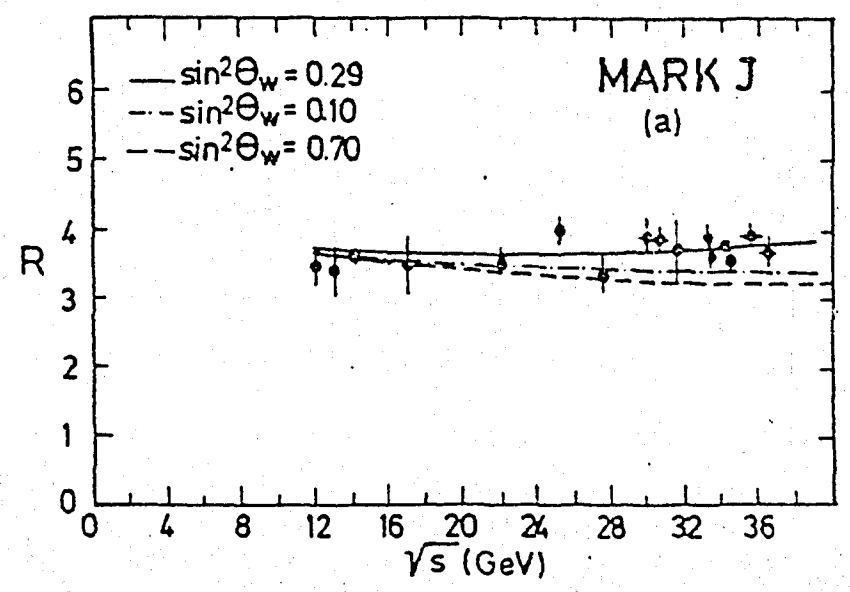

Figure 20. : R vs. $\sqrt{s}$ compared to predictions for various values of $\sin^2\theta_w$.

---

[15] D. P. Barber et al., (MARK-J Collaboration)Phys. Rev. Lett. 46 (1981) 1663. W. Bartel et al., (JADE Collaboration) Phys. Lett. 101B (1981) 361.

[16] W. Bartel et al., DESY REPORT 81-015 (1981).

3.2 BOUNDS ON WEAK ANGLES

By putting an upper limit on the B particle lifetime, measured in events containing muons, JADE has deduced[17] a limit on weak mixing angles. In their formalism, decays of a b quark to a u quark are proportional to $\sin(\beta)$ and decays to a c quark are proportional to $\sin(\gamma)\cos(\beta)$. The lifetime of the particle is then influenced by these angles, being longer if both $\sin(\gamma)$ and $\sin(\beta)$ are small. Figure 21 on page 223 shows their bounds on the angles derived from their determination that the lifetime is less than 1.4×10^{-12} sec. The upper limit on the angles comes from high accuracy measurements of the Cabibbo angle in different processes. Since the figure is drawn on a log scale, it should be noted that there is still substantial freedom for these angles.

3.3 PRODUCTION OF LEPTONS IN HADRONIC EVENTS

The leptons in hadronic events can give us much information about the electroweak production of heavy quarks and about their weak decays. An experimental program to understand these leptons is under way at PETRA. The primary goal of this is to measure the forward-backward charge asymmetry in the production of heavy quark pairs. Since this asymmetry is inversely proportional to the quark charge, the asymmetry expected for charmed quark production is 50% larger than for muon pairs and the asymmetry for bottom is a factor of three larger. The asymmetry in the production of heavy quarks is transmitted into the charge asymmetry in their decay muons.

Of course the leptons from heavy quark decay may allow us to measure several other quantities of interest, such as the charm and bottom fragmentation functions and the semileptonic decay branching ratios for charm and for bottom. I will report on a preliminary determination of the semileptonic branching ratio for bottom to indicate how the charm and bottom flavors can be separated even at high energy.

First, to show that the fragmentation functions can be tuned up to fit the data, the momentum distribution of muons in hadron events is shown in Figure 22 on page 224. The detector used, MARK-J, has a minimum momentum cut off of around 1.3 GeV imposed by the requirement that a muon, to be identified, must pass through the entire hadron calorimeter and be momentum analysed using the outside muon chambers.

---

[17] W. Bartel et al., DESY REPORT 82-014 (1982).

To make a partial separation of the muons from bottom decay, we look at the transverse momentum of the muons with respect to the jet axis of the jet containing the muon. Since transverse momentum due to fragmentation is small, the muon transverse momentum will largely come from the kick received in the decay of the massive parent particle. For a B particle decay, the average transverse momentum is considerable, around 1 GeV. In Figure 23 on page 225, the Monte Carlo P_T distribution of muons from three sources is shown. Although the B decay events are only a small part of the inclusive muon event sample, when a cut of $P_T > 1.2$ GeV is applied, we find that we can enrich the fraction from bottom to 45% of the total. This means we can use the rate of events with P_T greater than 1.2 GeV to measure the bottom semileptonic branching ratio. In Figure 24 on page 226, the measured P_T distribution is compared to what we expect according to the Monte Carlo, assuming a $B \rightarrow \mu + X$ branching ratio of 8%. The agreement over the entire distribution is quite good. Using the rate for $P_T > 1.2$ GeV then, we find

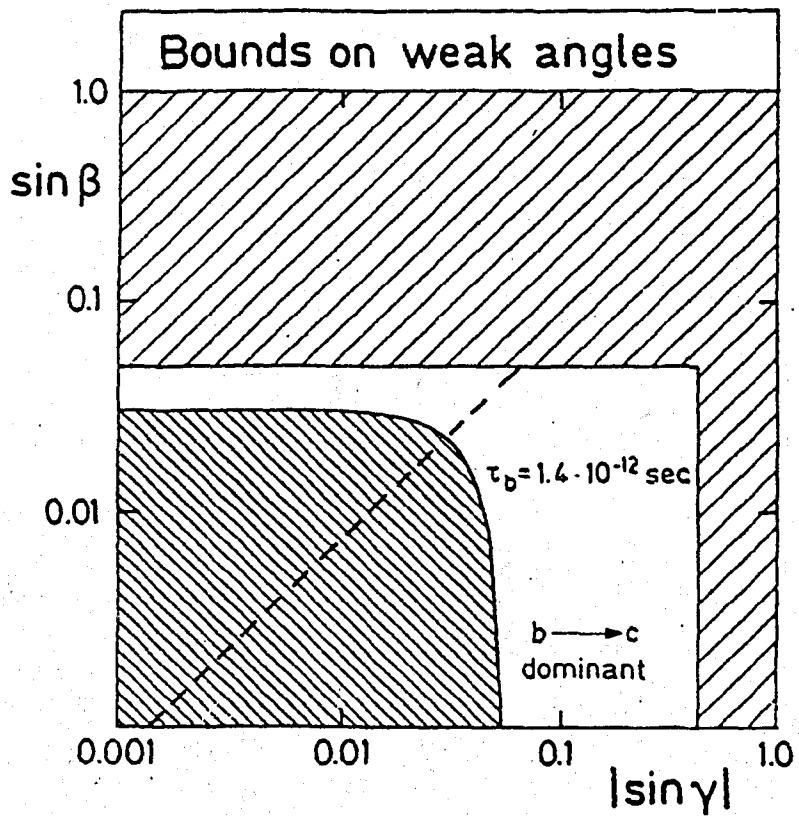

Figure 21. : Bounds placed on Miani angles by JADE's limit on the B particle lifetime.

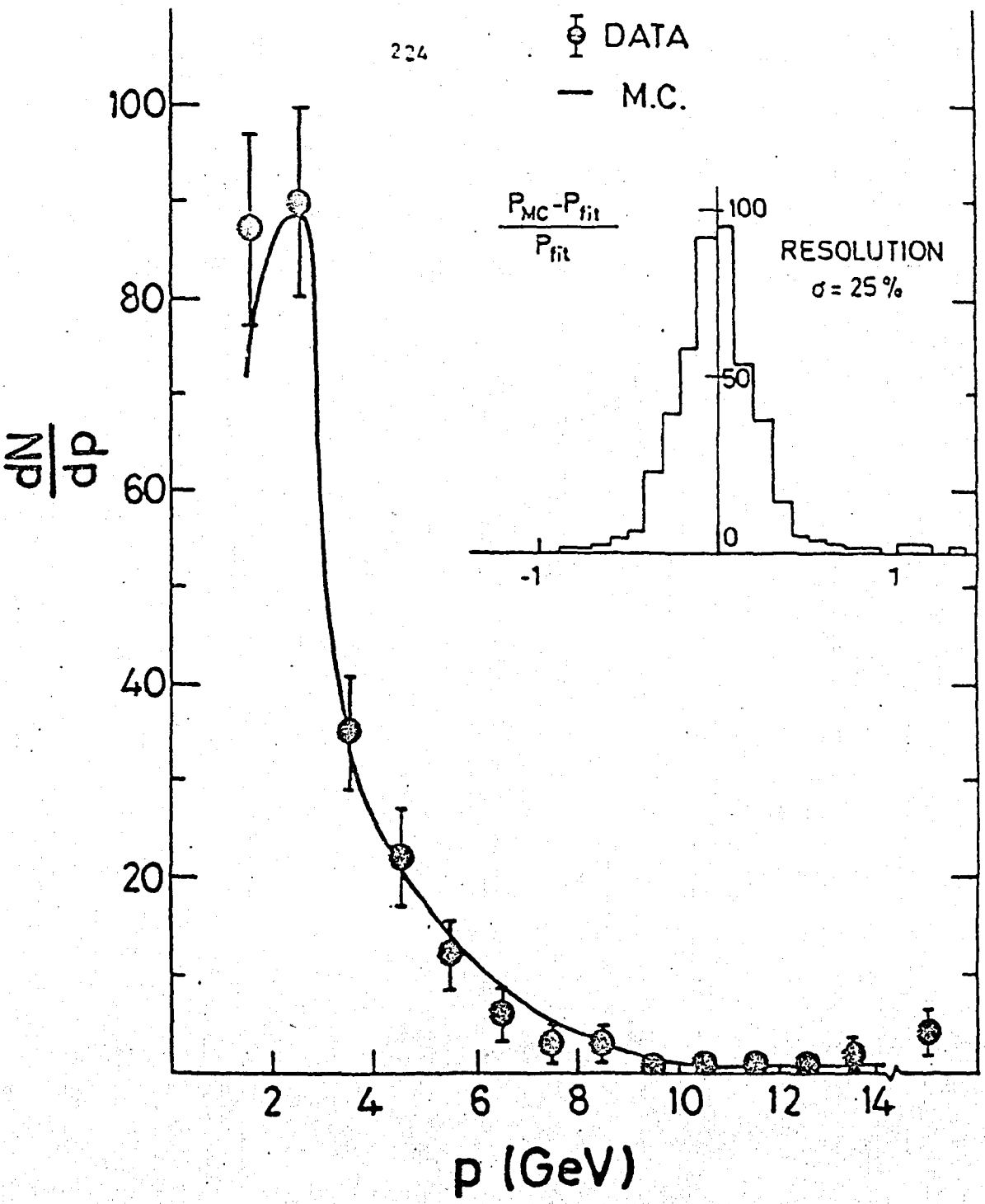

Figure 22. : Momentum distribution of muons found in hadron events compared to Monte Carlo.

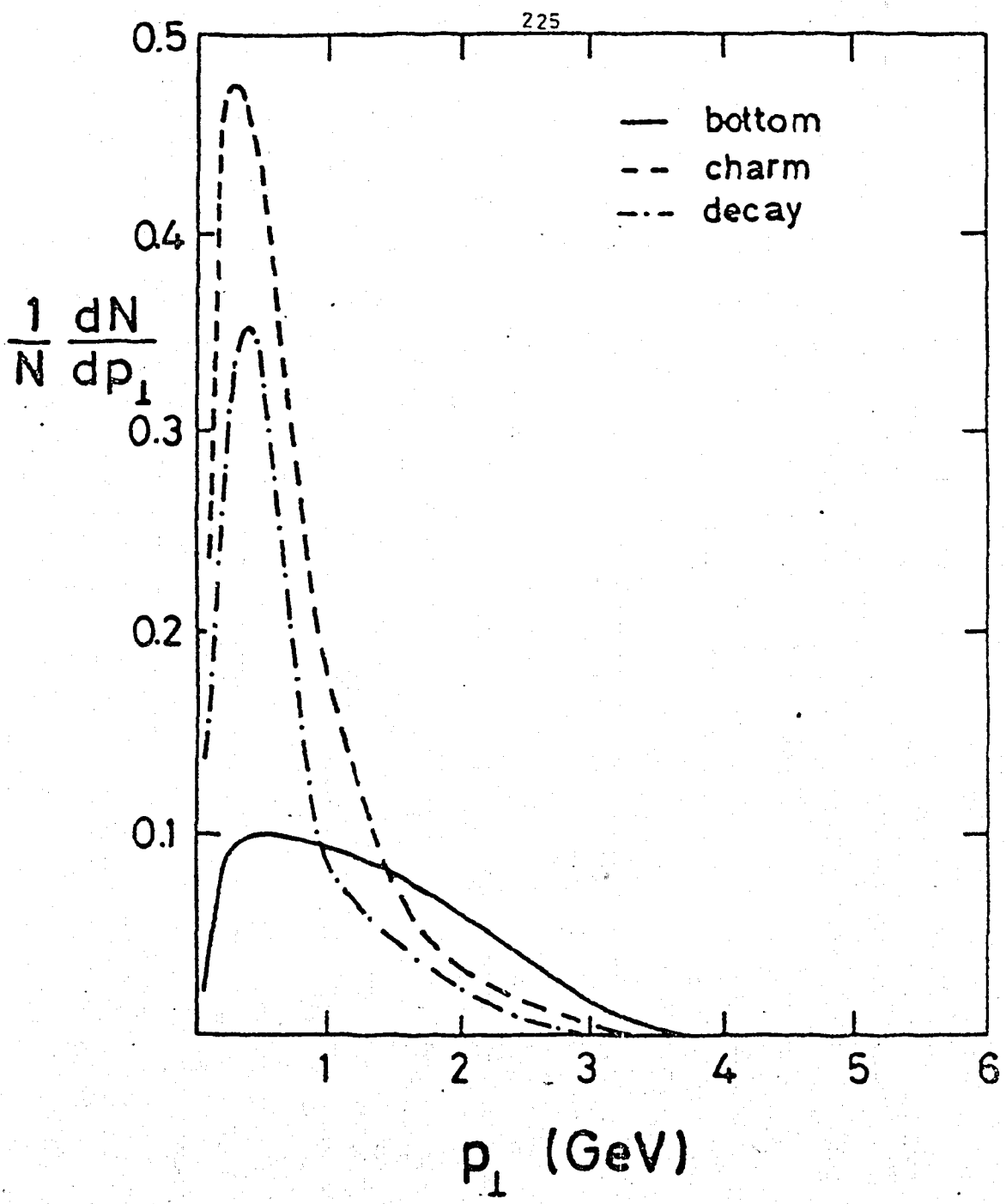

Figure 23. : Transverse momentum distribution from muons in hadron events according to Monte Carlo from charm decay, bottom decay and background.

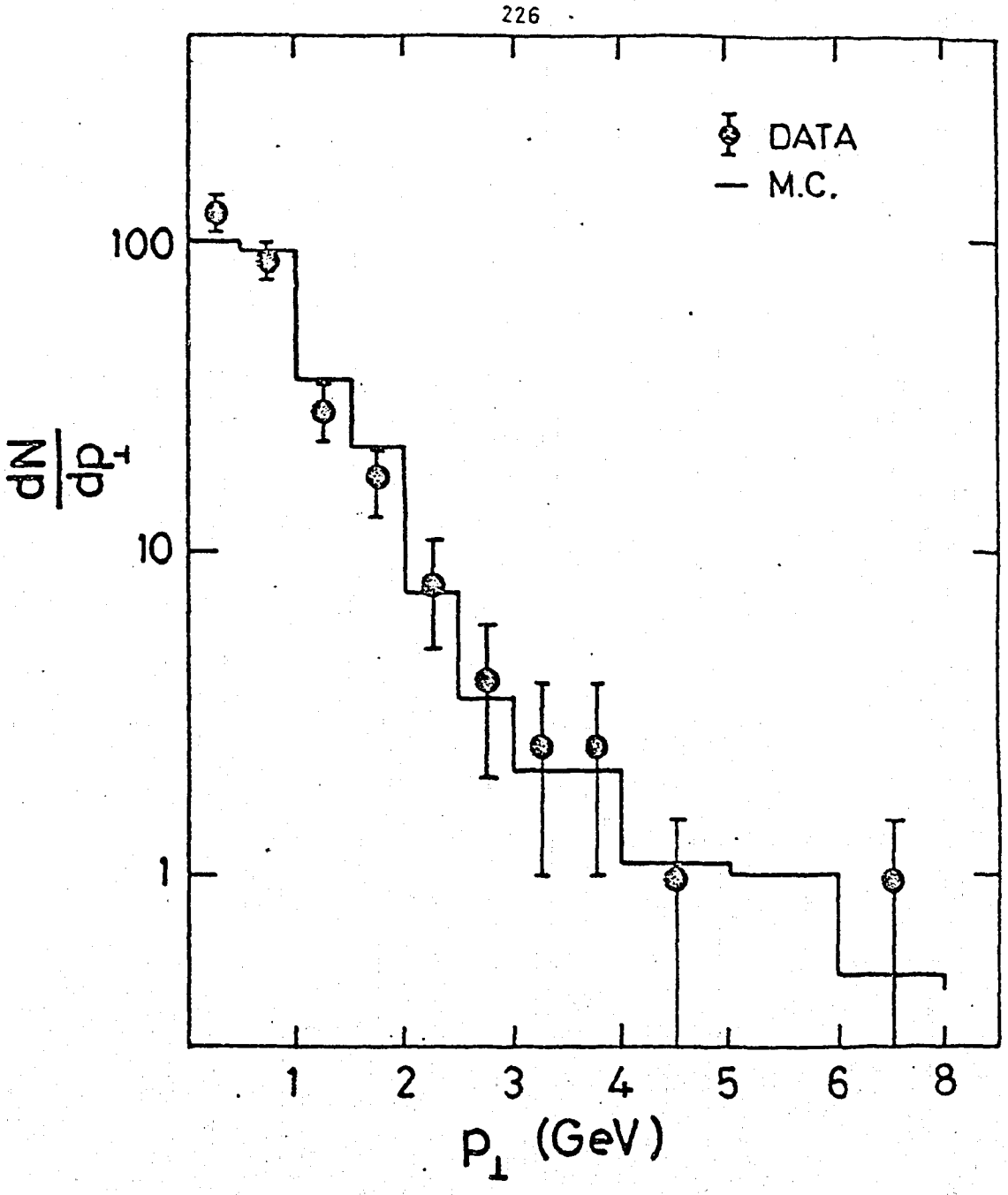

Figure 24. : Transverse momentum distribution from muons in hadron events. Monte Carlo expectation is shown as the solid line.

$$\text{Br}(B \to \mu + X) = 8.1\% \pm 3.3\% \text{ statistical} \pm 2.0\% \text{ systematic}$$

$$\text{Br}(C \to \mu + X) = 8.3\% \pm 1.4\% \text{ statistical} \pm 2.0\% \text{ systematic}$$

where this branching ratio refers only to the primary decay of a B particle to a muon, not to muons from the cascade decay through charm.

With this separation between b and c quarks, we can try to measure the heavy quark production asymmetry. This is hampered by the fact that the muons from c decay are expected to have an asymmetry of opposite sign to that from b decay. Thus, unless the separtion can be made very clearly, the large expected asymmetry will be watered down by background. The situation for the b asymmetry is even slightly worse than that because the muons from the cascade decay $b \to c \to \mu$ also tend to cancel the asymmetry in $b \to \mu$. Present results on asymmetry measurements from MARK-J are shown in table IV.

TABLE IV

MEASURED ASYMMETRIES IN B AND C SAMPLES

q	A measured	A expected	A original
b	- 9 ± 13%	- 6%	-27%
c	+ 4 ± 6%	+ 5%	+14%

It can be seen that better flavor identification methods must be found in order to accurately measure the heavy quark couplings. One way to do this may be through use of a high precision vertex chamber to identify charm decay vertices.

4.0 SEARCH FOR STRUCTURE IN THE FERMIONS

The data presented previously, on production of charged leptons, can be used to search for structure in the fermion by looking for a q^2 dependence to the cross sections that is not expected. In this measurement, we assume that the standard weak model is correct or at least that weak effects are nearly as small as in the standard model. One new item of data is shown in Figure 25 on page229. Here the measurements of R are used to look for structure in the quarks. A breakdown of the pointlike behavior of any of the fermions is parameterized in terms of a form factor with one parameter, Λ[18].

$$F_{\pm} = 1 \mp \frac{q^2}{q^2-\Lambda_{\pm}^2}$$

The + and - refer to two different form factors, one of which increases the cross sections and one of which decreases them. Table V lists the 95% confidence level lower limits for the Λ parameters.

---

[18] S. D. Drell, Ann. Phys. 4 (1958) 75.

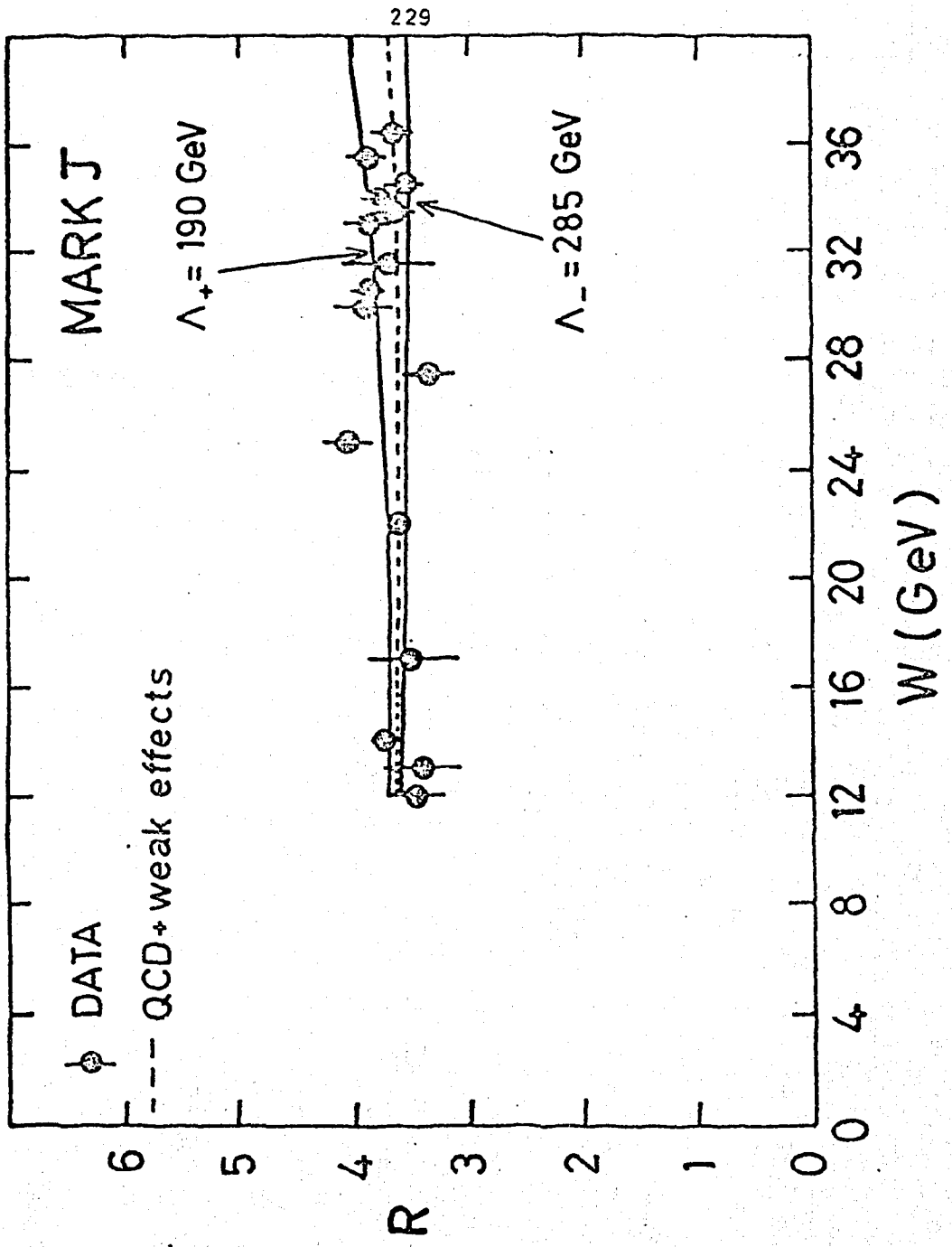

Figure 25. : MARK-J measurements of R compared to expectation with nonpointlike quark behavior.

TABLE V

95% C.L. LOWER LIMITS OF Λ_+

	e		μ		τ		q	
	Λ_+	Λ_-	Λ_+	Λ_-	Λ_+	Λ_-	Λ_+	Λ_-
CELLO	83	155	186	101	139	120		
JADE	112	106	142	126	111	93		
MARK-J	128	161	194	153	126	116	190	285
PLUTO	80	234	107	101	79	63		
TASSO	140	296	136	281	124	104		186

None of the fermions show evidence of structure up to energy scales of around 150 GeV.

Another way to look for structure is to look for excited states of the fermions. This has been done for the electron and muon.
A heavy electron[19] would influence the process

$$e^+e^- \rightarrow \gamma\,\gamma$$

by adding an extra diagram containing a virtual e*. The coupling at the e^+-e* vertex is, however, a free parameter which depends on the nature of the excited state. We assume a coupling constant λ which is dimensionless as it is a ratio to e. Figure 26 on page 231 shows that the limits placed by the measurement of $e^+e^- \rightarrow \gamma\gamma$. The line is a 95% confidence level limit, the region to the left of the line is forbidden. Previous limits assuming that

[19] A. Litke, Harvard University, Ph.D. Thesis (1970), unpublished.

$s << M_{e^*}^2$ are shown as limits on the e^* mass near $\lambda = 1$ to which they roughly correspond.

An excited muon has been looked for in two production processes.

$$e^+e^- \longrightarrow \mu^{*+}\ \mu^{*-} \longrightarrow \mu^+\ \mu^-\ \gamma\ \gamma$$

$$e^+e^- \longrightarrow \mu^*\ \mu \longrightarrow \mu^+\ \mu^-\ \gamma$$

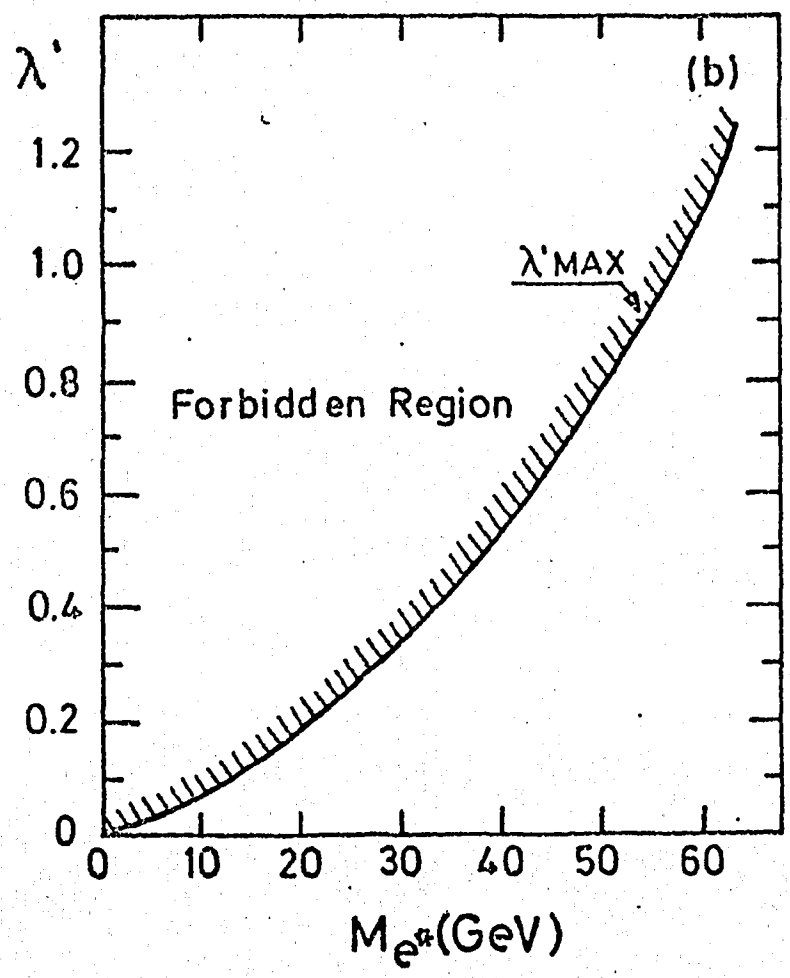

Figure 26. : Limit on excited electron coupling constant as a function of its mass.

SEARCH FOR STRUCTURE IN THE FERMIONS

In the first process, the coupling is near to that for production of any charged fermion, so absolute limits can be placed in the mass. This puts a limit on the mass

$$M_{\mu^*} > 10 \text{ GeV}.$$

In the second process, again the coupling at the vertex is not known Figure 27 shows the 95% confidence level limit on λ^2 and M_{μ^*} Also shown is the limit on the ratio of $\sigma_{\mu^*\mu}/\sigma_{\mu\mu}$This ratio is limited to only a few percent.

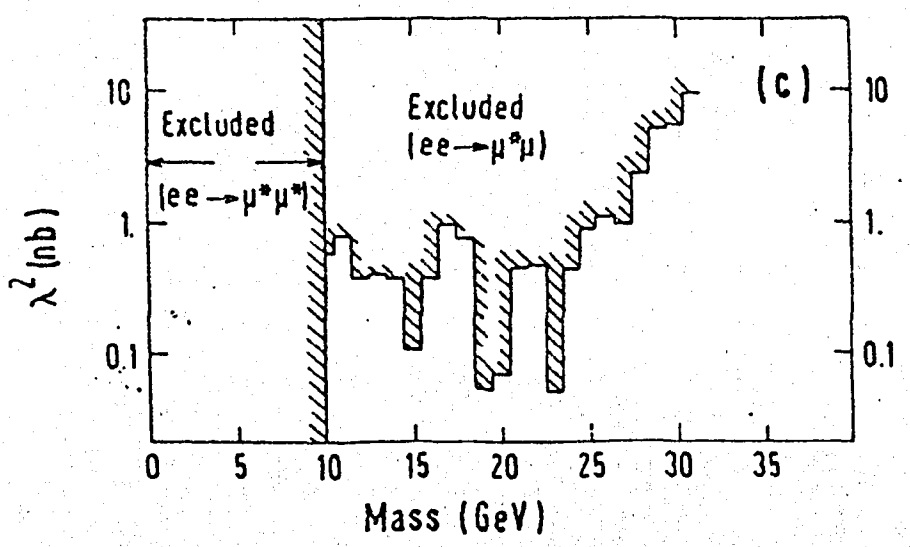

Figure 27. : Limit on excited muon couling constant as a function of its mass.

5.0 SEARCH FOR SYMMETRY BREAKING SCALARS

Of course an important aspect of the present weak interaction theory is spontaneous symmetry breaking by the Higgs mechanism. The standard model predicts that there should be an observable neutral scalar particle. As yet, no such particle has been found nor have any strigent limits been placed on its mass. This may become possible if the top threshold is reached and the Higgs particle can be searched for in production by the Wilcek mechanism[20].

The method of symmetry breaking in elementary particle physics remains a mystery. Symmetry breaking is though to be responsible for the generation of all fundemental particle masses, the weak mixing angles among quark species, CP violation and perhaps for the large parity violation seen in weak interactions. Among proposed forms of symmetry breaking, one prediction is universal. That is the existence of new scalar particle, be they Higgs particles, technipions or supersymmetric scalar partners of fermions.

In the standard model, Higgs couplings to each fermion are independently free parameters which must be set to generate the fermion masses. More ambitious theories have been put foreward to explain the spontaneous symmetry breaking of SU(2)×U(1) and the fermion mass generation. In grand unified theories, symmetry breaking is performed by a large number of Higgs particles some of which are charged. Although many of the Higgs particles are superheavy, some may have masses on the order of 10 GeV. Technicolor[21] [22] models, in which the symmetry breaking scalars are composed of constituents confined by a new strong force (technicolor), predict the existence of reasonably light charged particles called

---

[20] F. Wilcek, Phys. Rev. Lett. 39 (1977) 1304.

[21] J. Schwinger, Phy. Rev. 125 (1962) 397, 128 (1969) 2425. R. Jackiw and K. Johnson, Phys. Rev. D8 (1973) 2386. J. M. Cornwall and R. E. Norton, Phys. Rev. D8 (1973) 3338. M. A. B. Bég and A. Sirlin, Ann. Rev. Nucl. Sci. 24 (1974) 379. S. Weinberg, Phys. Rev. D13 (1976) 974, D19 (1979) 1277. L. Susskind, Phys. Rev. D20 (1979) 2619.

[22] For review, see K. D. Lane and M. E. Peskin, Rencontre de Moriond Lectures, NORDITA preprint 80/33 (1980). E. Farhi and L. Susskind, CERN preprint TH. 2975 (1980). P. Sikivie, Rencontre de Moriond Lecture, CERN preprint TH. 3083 (1981), and contributions to Proc. Cornell Z_0 Theory Workshop, Eds. M. E. Peskin and S. H. H. Tye, CLNS 81-485 by S. H. H. Tye, p. 411; E. Eichten, p. 421; A. Ali, DESY preprint 81/032 presented at Orbis Scientiae, Coral Gables (1981). M. A. B. Bég, Rockerfeller University preprint RU81/B/9 presented at the Lisbon International Conference on High Energy Physics (1981).

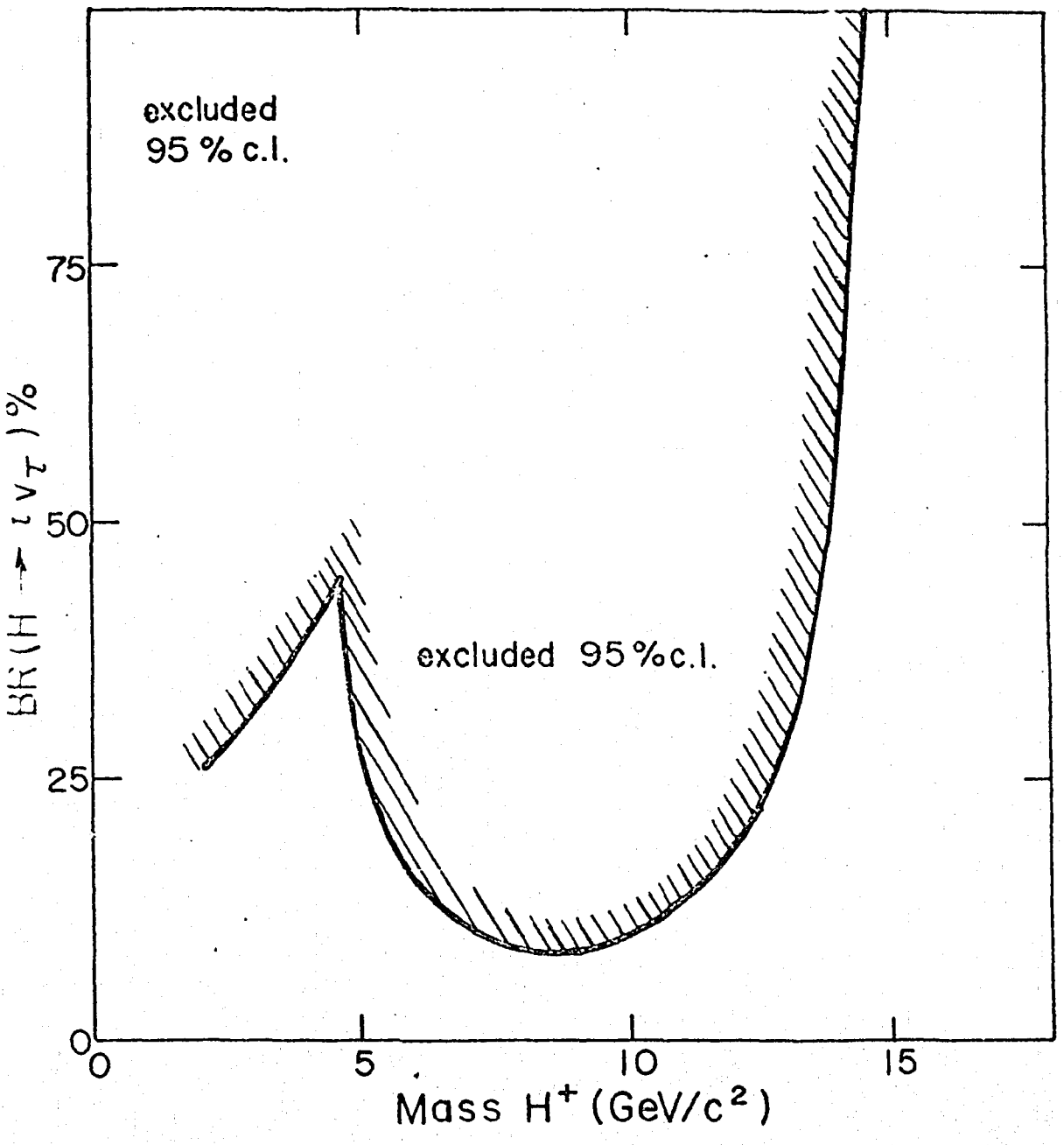

Figure 28. : Limit on mass and branching ratio into $\tau\nu$ for technipion or charged Higgs from MARK-J.

SEARCH FOR SYMMETRY BREAKING SCALARS

technipions. Since these are charged, they will be produced in e^+e^- annihilations through one photon. This implies $\Delta R=1/4$ when well above threshold. In fact there are some specific technicolor models[23] which predict that the technipion mass lies between 5 and 14 GeV, which is the range that we can most easily explore at PETRA.

Figure 28 on page 234 and Figure 29 show two searches for technipion or charged Higgs production. Since both of these particles should be produced at the same rate and both decay primarily into the heaviest fermion antifermion pairs allowed by energy conservation, they may be studied simultaneously. In the mass range explored, the decay modes will be mainly $\bar{\tau}\nu$ and $c\bar{s}$. The branching ratio between these two modes depends on the specific theory. We have therefore left it, along with the technipion or Higgs mass, as a free parameter. Decays to a $c\bar{b}$ pair are

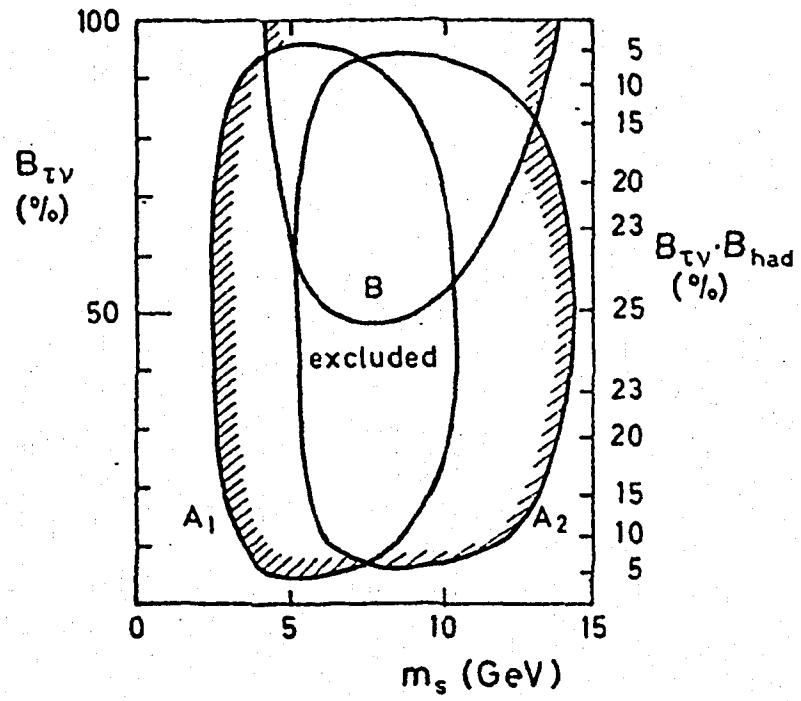

Figure 29. : Limit on mass and branching ratio into $\tau\nu$ for technipion or charged Higgs from JADE.

---

[23] S. Dimopoulos, S. Raby, and G. L. Kane, Nucl. Phys. B182, 77 (1981) S. Chadha and M. E. Peskin, Nucl. Phys. B185, 61 (1981). S. Chadha and M. E. Peskin, Nucl. Phys. B187, 541 (1981).

found to give tighter limits than the $c\bar{s}$ decay. In the figures, the regions in the plane defined by the charged scalar mass and its branching ratio into the $\bar{\tau}\nu$ mode which are excluded at the 95% confidence level are displayed. Except for very small branching fractions to $\bar{\tau}\nu_\tau$, these scalars are excluded in the 4 to 15 GeV mass range. In supersymmetric grand unified theories, there is a symmetry between bosons and fermions that requires that each fermion have two scalar partners that are symmetrically associated with it. In our search for these scalars, we assume[24] that they decay rapidly into their fermion partner plus unobserved photinos or goldstinos. Mass limits[25] for scalar partners of the electron, muon and tau have been obtained by PETRA experiments and are shown in table VI.

TABLE VI

LIMITS IN SUPERSYMMETRIC PARTNERS OF LEPTONS

s_e	$m > 16$ GeV
s_μ	$m > 16$ GeV
s_τ	$m > 14$ GeV

[24] P. Fayet, CERN-Report TH-2864 (1980).

[25] J. Burger, Proc. Int. Symp. Lepton and Photon Interactions at High Energy (Bonn, 1981). D. P. Barber et al., Phys. Rev. Lett. 45, 1904 (1980). D. P. Barber et al., MIT/LNS-125 (1982).

6.0 SUMMARY

Weak effects have been observed for the first time at PETRA in the forward-backward asymmetry in muon pair production.

$$A_{\mu\mu} = -11.9\% \pm 1.6\% \text{ expecting } -8.7\%$$

The expectation is that from the Glashow-Weinberg-Salam model. The highest q^2 test of the model lends strong support to the existence of the Z_0 boson with a mass limited to be between 49 and 95 GeV at the 95% confidence level. The charged lepton coupling constants g_A and g_V have been measured in purely leptonic processes at high q^2 and are found to be in agreement with the predictions of the standard theory and also with the low q^2 measurements in neutrino electron scattering.

$$|g_A| \approx 0.50$$
$$|g_V| \approx 0.0$$

A limit on more general weak interaction models has been made in terms of the normalized difference between the real theory and the standard theory.

$$C < 0.027$$

This limit is of interest to any model with more neutral currect structure than a single Z_0 boson.

Using quarks along with the leptons we have made a high q^2 measurement of $\sin^2\theta_w$

$$\sin^2\theta_w = 0.27 \begin{matrix} +0.06 \\ -0.04 \end{matrix}$$

We have begun to look at the weak interactions of the heavy quarks. A first result is found that

$$\text{Br}\,(B \to \mu + X) = 8.1\% \pm 3.3\% \pm 2\%$$
$$\text{Br}\,(C \to \mu + X) = 8.3\% \pm 1.4\% \pm 2\%$$

where the second error is systematic.

We find that the fermions are pointlike with no evidence of structure up to the energy scale of 100-200 GeV.

SUMMARY